Journal of Electronic Imaging 11(3), 316–337 (July 2002).

Analysis of the microstructures ("rosettes") in the superposition of periodic layers

Isaac Amidror
Roger D. Hersch
Ecole Polytechnique Fédérale de Lausanne (EPFL)
Lab. de Systèmes Périphériques (LSP)
1015 Lausanne, Switzerland

Abstract. *Superpositions of periodic dot screens are largely used in electronic imaging in the field of color printing. In such superpositions the interaction between the superposed layers may cause new structures to appear which did not exist in any of the original layers: macrostructures (also known as moiré patterns) and microstructures (also known as rosettes). While macrostructures are not always generated in the superposition (cf. moiré-free superpositions), microstructures exist practically in any superposition, except for the most trivial cases. In fact, even the macrostructures, whenever they occur, consist of variations in the microstructure of the superposition. In the present paper we investigate the microstructures that appear in the superposition of periodic structures and their properties. We also find the conditions on the superposed layers under which the microstructure of the superposition varies—or remains invariant—when individual layers in the superposition are laterally shifted with respect to each other.* © *2002 SPIE and IS&T.*
[DOI: 10.1117/1.1477442]

1 Introduction

When periodic layers (line gratings, dot screens, etc.) are superposed, new structures of two distinct levels may appear in the superposition, which do not exist in any of the original layers: *macrostructures* and *microstructures*.

The macrostructures, usually known as *moiré patterns*, are much coarser than the detail of the original layers, and they are clearly visible even when observed from a distance. The microstructures, on the contrary, are almost as small as the periods of the original layers (typically, just 2–5 times larger), and, therefore, they are only visible when examining the superposition from a close distance or through a magnifying glass. These tiny structures are also called *rosettes* owing to the various flower-like shapes they often form in the superposition of dot screens (Ref. 1, p. 339).

While macrostructures (moiré effects) have been treated over the years in a large number of references (see, for example, in Refs. 2 and 3), only a few studies have been devoted to the microstructures. However, in spite of their tiny size, the microstructures which occur in the superposition are very rich in detail, and their study appears to be not less fascinating than the study of the macrostructures. As we can see in Fig. 1, quite attractive rosette forms often appear in the superposition, and a look through a magnifying glass may reveal an amazing, subtle, and delicate microworld, full of surprising geometrical forms.

We will see in this paper that macrostructures and microstructures may coexist in the same superposition. However, while microstructures exist practically in any superposition, except for the most trivial cases, macro moiré effects are not always present (cf. stable and unstable moiré-free states in Sec. 2.3 below). In fact, we will see in Sec. 4.1 that the macrostructures, whenever they exist, are constructed from the microstructures of the superposition.

In the present paper we investigate the microstructures generated in the superposition of periodic layers and their properties both in the image domain and in the spectral domain. Our approach is completely general, and not only limited to the rosette morphology in the classical case used for color printing, the superposition of three screens 30° or 60° apart, which has already been studied in Ref. 1, Ref. 4, pp. 57–59, and Ref. 5. We start in Sec. 2 by establishing the required terminology and mathematical framework for the rest of the paper. We then discuss the behavior of the microstructure in all the different types of superpositions: singular superpositions in Sec. 3, and nonsingular superpositions in Sec. 4. Then, in the remaining sections we proceed to the formal explanation of these phenomena. This also leads us to new, general results concerning the stability of the microstructure under layer shifts in the superposition. We show that shifts of individual layers substantially change the microstructure of the superposition (e.g., from dot-centered rosettes to clear-centered rosettes or vice versa) if and only if the superposition is singular. Several figures and examples taken from the printing world illustrate our discussion throughout the paper.

2 Background and Basic Notions

In this introductory section we briefly review the basic notions and terminology that will be used throughout this paper.

2.1 *Properties of the Superposed Layers and Their Fourier Spectra*

First of all, let us mention that throughout this work we are only concerned with monochrome, black and white images

Paper JEI 99073 received Dec. 6, 1999; revised manuscript received Jun. 28, 2001; accepted for publication Dec. 7, 2001.
1017-9909/2002/$15.00 © 2002 SPIE and IS&T.

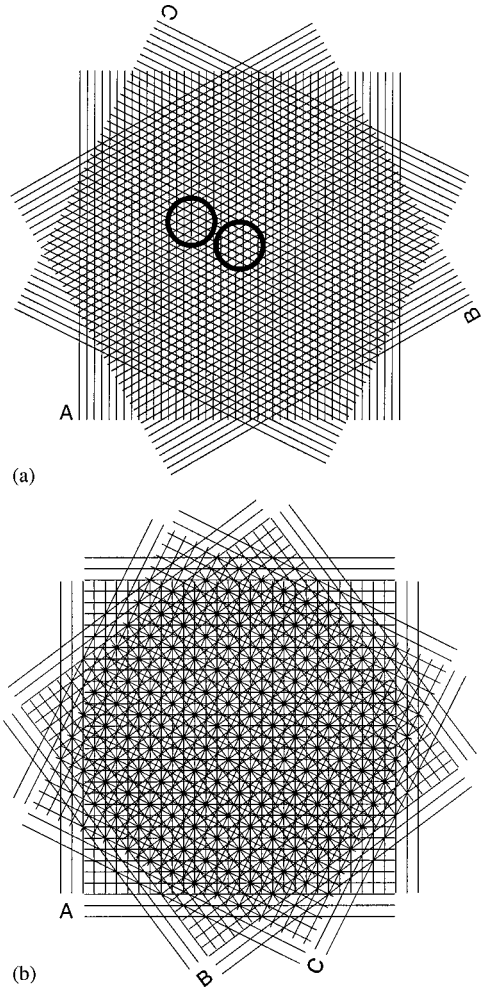

Fig. 1 The superposition of periodic layers may yield very spectacular microstructures (rosettes). (a) A magnification of the three-grating superposition of Fig. 4(h). Note the star-like rosettes which form the bright areas of the macromoiré and the triangular microstructure which forms the darker areas. (b) A magnification of a singular superposition of three grids (=6 gratings) with angles $\theta_1=0°$, $\theta_2=36.8699°$, $\theta_3=63.4349°$, and periods $T_1=T_2$, $T_3=1.118T_1$. This is an example of a periodic, singular superposition (Sec. 3.1).

(or ''layers''). This means that each image can be represented by a *reflectance* function, which assigns to any point (x,y) of the image a value between 0 and 1 representing its light reflectance: 0 for black (i.e., no reflected light), 1 for white (i.e., full light reflectance), and intermediate values for in-between shades. In the case of transparencies, the reflectance function is replaced by a *transmittance* function defined in a similar way. The superposition of such images can be done by overprinting, or by laying printed transparencies on top of each other. Since the superposition of black and any other shade always gives black, this suggests a *multiplicative* model for the superposition of monochrome images. Thus, when m monochrome images are superposed, the reflectance of the resulting image is given by the *product* of the reflectance functions of the individual images

$$r(x,y)=r_1(x,y)r_2(x,y)\ldots r_m(x,y). \tag{1}$$

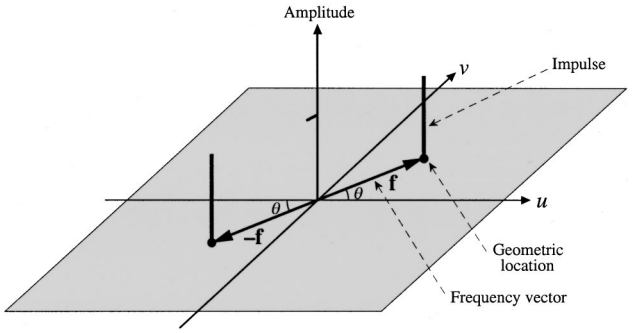

Fig. 2 The *geometric location and amplitude* of impulses in the 2D spectrum. To each impulse is attached its *frequency vector*, which points to the geometric location of the impulse in the spectrum plane (u,v).

According to the convolution theorem (Ref. 6, p. 244) the Fourier transform of the product function is the convolution of the Fourier transforms of the individual functions. Therefore, if we denote the Fourier transform of each function by the respective capital letter and the two-dimensional (2D) convolution by $**$, the spectrum of the superposition is given by

$$R(u,v)=R_1(u,v)**R_2(u,v)**\ldots**R_m(u,v). \tag{2}$$

Second, we are basically interested in *periodic* images defined on the continuous (x,y) plane, such as line gratings or dot screens, and their superpositions. This implies that the spectrum of the image on the (u,v) plane is not a continuous one but rather consists of impulses, corresponding to the frequencies which appear in the Fourier series decomposition of the image (Ref. 6, p. 204). In the case of a onefold periodic image, such as a line grating, the spectrum consists of a one-dimensional (1D) ''comb'' of impulses centered on the origin; in the case of a twofold periodic image the spectrum is a 2D ''nail bed'' of impulses centered on the origin. Note that we will sometimes use the more general term ''cluster'' for a comb or a nail bed; this should not be confused, however, with terms such as ''clustered dot halftoning,'' etc.

Each impulse in the 2D spectrum is characterized by three main properties: its *label* (which is its index in the Fourier series development); its *geometric location* (or *impulse location*), and its *amplitude* (see Fig. 2). To the geometric location of any impulse is attached a *frequency vector* **f** in the spectrum plane, which connects the spectrum origin to the geometric location of the impulse. This vector can be expressed either by its polar coordinates (f,θ), where θ is the direction of the impulse and f is its distance from the origin (i.e., its frequency in that direction); or by its Cartesian coordinates (f_u,f_v), where f_u and f_v are the horizontal and vertical components of the frequency. In terms of the original image, the *geometric location* of an impulse in the spectrum determines the frequency f and the direction θ of the corresponding periodic component in the image, and the *amplitude* of the impulse represents the intensity of that periodic component in the image. (Note that if the original image is not symmetric about the origin, the amplitude of each impulse in the spectrum may also have a nonzero imaginary component).

However, the question of whether or not an impulse in the spectrum represents a *visible* periodic component in the image strongly depends on properties of the human visual system. The fact that the eye cannot distinguish fine details above a certain frequency (i.e., below a certain period) suggests that the human visual system model includes a low-pass filtering stage. This is a bidimensional bell-shaped filter whose form is anisotropic (since it appears that the eye is less sensitive to small details in diagonal directions such as 45°).[7] However, for the sake of simplicity this low-pass filter can be approximated by the *visibility circle*, a circular step function around the spectrum origin whose radius represents the *cutoff frequency* (i.e., the threshold frequency beyond which fine detail is no longer detected by the eye). Obviously, its radius depends on several factors such as the contrast of the observed details, the viewing distance, light conditions, etc. If the frequencies of the original image elements are beyond the border of the visibility circle in the spectrum, the eye can no longer see them; but if a strong enough impulse in the spectrum of the image superposition falls inside the visibility circle, then a moiré effect becomes visible in the superposed image. (In fact, the visibility circle has a hole in its center, since very low frequencies cannot be seen, either.)

For the sake of convenience, we may assume that the given images (gratings, grids, etc.) are symmetrically centered about the origin. As a result, we will normally deal with images (and image superpositions) which are *real* and *symmetric*, and whose spectra are, consequently, also real and symmetric (Ref. 6, pp. 14, 15). This means that each impulse in the spectrum (except for the dc impulse at the origin) is always accompanied by a twin impulse of an identical amplitude, which is symmetrically located at the other side of the origin as in Fig. 2 (their frequency vectors are $\mathbf{f}$ and $-\mathbf{f}$). If the image is nonsymmetric (but, of course, still real), the amplitudes of the twin impulses at $\mathbf{f}$ and $-\mathbf{f}$ are complex conjugates.

2.2 *Spectrum Convolution and Superposition Moirés*

According to the convolution theorem [Eqs. (1), (2)], when m line gratings are superposed in the image domain, the resulting spectrum is the convolution of their individual spectra. This convolution of combs can be seen as an operation in which frequency vectors from the individual spectra are added vectorially, while the corresponding impulse amplitudes are multiplied. More precisely, each impulse in the spectrum convolution is generated during the convolution process by the contribution of *one* impulse from *each* individual spectrum: its location is given by the sum of their frequency vectors, and its amplitude is given by the product of their amplitudes. This permits us to introduce an indexing method for denoting each of the impulses of the spectrum convolution in a unique, unambiguous way. The general impulse in the spectrum convolution will be denoted the $(k_1,k_2,\ldots,k_m)$ *impulse*, where m is the number of superposed gratings, and each integer k_i is the index (harmonic), within the comb (the Fourier series) of the ith spectrum, of the impulse that this ith spectrum contributed to the impulse in question in the convolution. Using this formal notation we can, therefore, express the geometric location of the general $(k_1,k_2,\ldots,k_m)$ impulse in the spectrum convolution by the vectorial sum (or linear combination)

$$\mathbf{f}_{k_1,k_2,\ldots,k_m} = k_1\mathbf{f}_1 + k_2\mathbf{f}_2 + \ldots + k_m\mathbf{f}_m \tag{3}$$

and its amplitude by

$$a_{k_1,k_2,\ldots,k_m} = {a^{(1)}}_{k_1}{a^{(2)}}_{k_2}\ldots{a^{(m)}}_{k_m}, \tag{4}$$

where $\mathbf{f}_i$ denotes the frequency vector of the fundamental impulse in the spectrum of the ith grating, and $k_i\mathbf{f}_i$ and ${a^{(i)}}_{k_i}$ are, respectively, the frequency vector and the amplitude of the k_ith harmonic impulse in the spectrum of the ith grating.

The vectorial sum of Eq. (3) can also be written in terms of its Cartesian components. If f_i are the frequencies of the m original gratings and θ_i are the angles that they form with the positive horizontal axis, then the coordinates (f_u,f_v) of the $(k_1,k_2,\ldots,k_m)$ impulse in the spectrum convolution are given by

$$\begin{aligned} f_{u_{k_1,k_2,\ldots k_m}} &= k_1 f_1 \cos\theta_1 + k_2 f_2 \cos\theta_2 + \ldots + k_m f_m \cos\theta_m, \\ f_{v_{k_1,k_2,\ldots,k_m}} &= k_1 f_1 \sin\theta_1 + k_2 f_2 \sin\theta_2 + \ldots + k_m f_m \sin\theta_m. \end{aligned} \tag{5}$$

Therefore, the frequency, the period, and the angle of the considered impulse (and of the moiré it represents) are given by the length and the direction of the vector $\mathbf{f}_{k_1,k_2,\ldots,k_m}$ as follows:

$$f = \sqrt{f_u^2 + f_v^2} \quad T_M = 1/f \quad \varphi_M = \arctan(f_v/f_u). \tag{6}$$

Let us now say a word about the notations used for the superposition moirés. We use a notational formulation which provides a systematic means for identifying the various moiré effects. As we have seen, a $(k_1,k_2,\ldots,k_m)$ impulse of the spectrum convolution which falls close to the spectrum origin, inside the visibility circle, represents a moiré effect in the superposed image (see Fig. 3). We call the m-grating moiré whose fundamental impulse is the $(k_1,k_2,\ldots,k_m)$ impulse in the spectrum convolution a $(k_1,k_2,\ldots,k_m)$ *moiré*; the highest absolute value in the index list is called the *order* of the moiré. Note that in the case of doubly periodic images, such as in dot screens, each image can be represented in the superposition by a pair of onefold periodic functions; hence, m in Eqs. (3)–(5) above counts each doubly periodic layer as two onefold periodic structures.

2.3 *Singular States; Stable Versus Unstable Moiré-Free Superpositions*

We have seen that if one or several of the new impulse pairs in the spectrum convolution fall close to the origin, inside the visibility circle, this implies the existence in the superposed image of one or several moirés with visible periods [see, for example, Figs. 3(c) and 3(f)]. An interesting special case occurs when some of the impulses of the convolution fall *exactly* on top of the dc impulse, at the

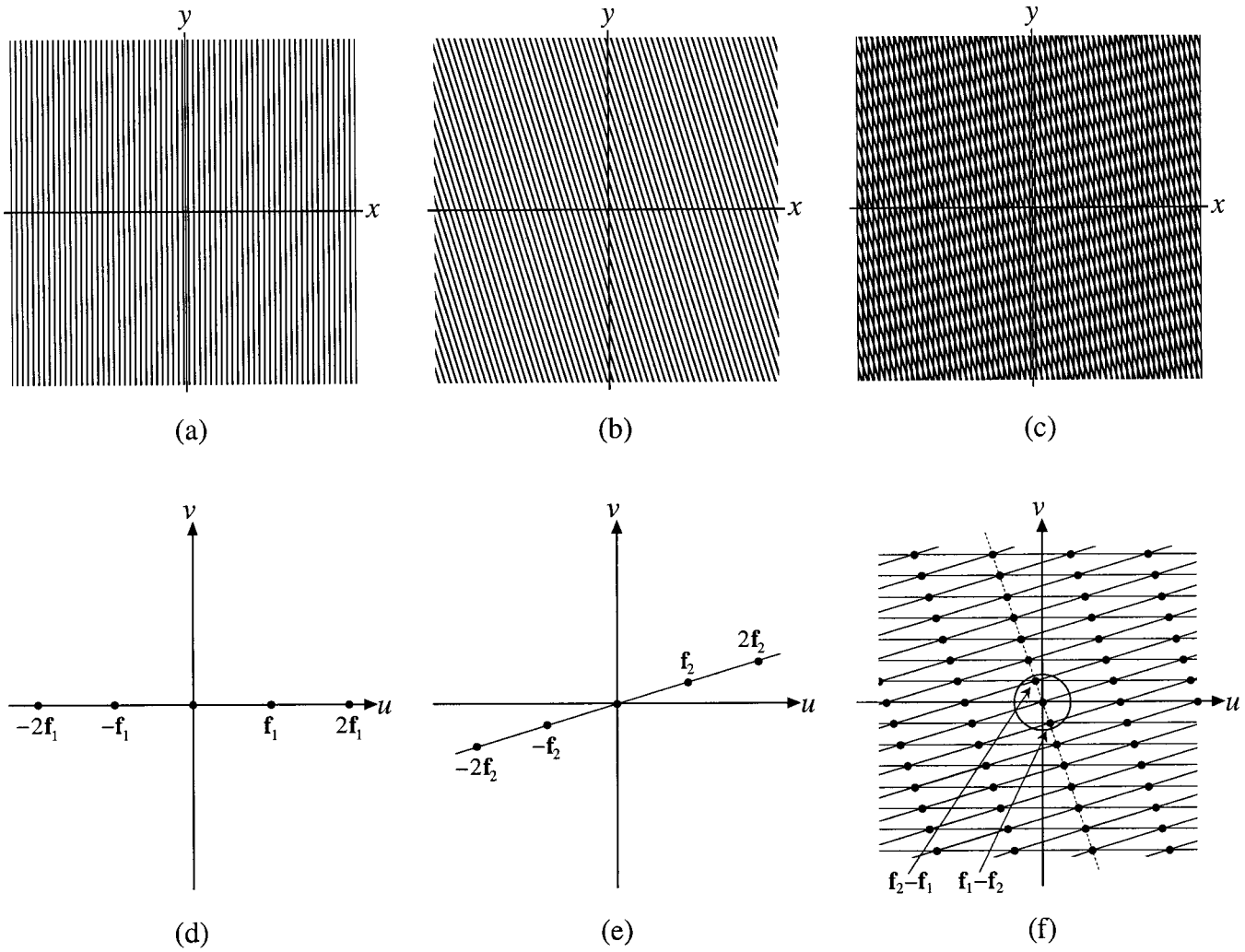

Fig. 3 Line gratings (a) and (b) and their superposition (c) in the image domain; their respective spectra are the infinite impulse combs shown in (d) and (e) and their convolution (f). Only impulse locations are shown in the spectra, but not their amplitudes. The circle in the center of the spectrum (f) represents the visibility circle. It contains the impulse pair whose frequency vectors are $\mathbf{f}_1-\mathbf{f}_2$ and $\mathbf{f}_2-\mathbf{f}_1$ and whose indices are $(1,-1)$ and $(-1,1)$; this is the fundamental impulse pair of the $(1,-1)$ moiré seen in (c). The dotted line in (f) shows the infinite impulse comb which represents this moiré.

spectrum origin. This happens, for instance, in the trivial superposition of two identical gratings in match, with an angle difference of 0° or 180°; or, more interestingly, when three identical gratings are superposed with angle differences of 120° between each other (see second and third rows of Fig. 4). As can be seen from the vector diagrams, these are limit cases in which the vectorial sum of the frequency vectors is exactly **0**. This means that the moiré frequency is 0 (i.e., its period is infinitely large), and, therefore, as shown in Figs. 4(d) and 4(g), the moiré is not visible. This situation is called a *singular moiré state*. But, although the moiré effect in a singular state is not visible, this is a very unstable moiré-free state, since any slight deviation in the angle or in the frequency of any of the superposed layers may cause the new impulses in the spectrum convolution to move slightly off the origin, thus causing the moiré to "come back from infinity" and to have a clearly visible period, as shown in Figs. 4(e) and 4(h).

It is important to understand, however, that not all the moiré-free superpositions are singular (and hence unstable). For example, the superposition of two identical gratings at an angle of 90° is indeed moiré free; however, it is not a singular state, but rather a *stable moiré-free state*: as shown in the first row of Fig. 4, no moiré becomes visible in this superposition even when a small deviation occurs in the angle or in the frequency of any of the layers. The corresponding situation in the spectral domain is clearly illustrated in Fig. 4(c), which shows the vector diagram of the superposition of Fig. 4(b).

Formally, we say that a singular moiré state occurs whenever a $(k_1,\ldots,k_m)$ impulse [other than (0,...,0)] in the spectrum convolution falls exactly on the spectrum origin, i.e., when the frequency vectors of the m superposed gratings, $\mathbf{f}_1,\ldots,\mathbf{f}_m$, are such that $\Sigma_{i=1}^{m} k_i\mathbf{f}_i=\mathbf{0}$. This implies, of course, that all the impulses of the $(k_1,\ldots,k_m)$-moiré comb

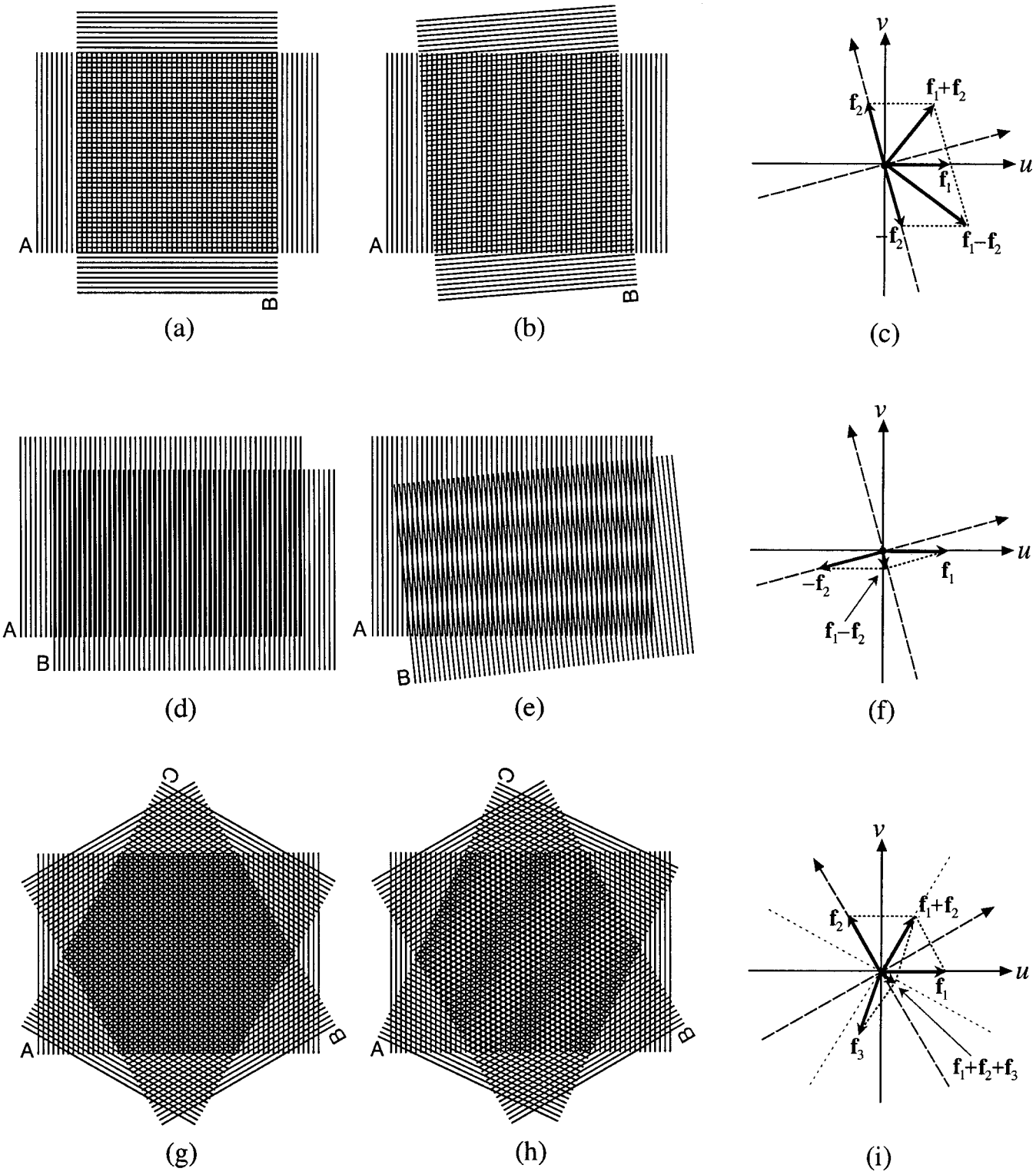

Fig. 4 Examples of stable and unstable (=singular) moiré-free states. First row: (a) the superposition of two identical gratings at an angle difference of 90° gives a stable moiré-free state; small angle or frequency deviations, as in (b), do not cause the appearance of any visible moiré. The spectral interpretation of (b) is shown in the vector diagram (c). Second row: (d) the superposition of two identical gratings at an angle difference of 0° gives a singular (unstable) moiré-free state. (e) A small angle or frequency deviation in any of the layers causes the reappearance of the moiré with a very significant visible period. The spectral interpretation of (e) is shown in the vector diagram (f); compare to Fig. 3(f) which also shows impulses of higher orders. Third row: (g) the superposition of three identical gratings with angle differences of 120° gives an unstable (singular) moiré-free state; again, any small angle or frequency deviation may cause the reappearance of a very significant moiré, as shown in (h) and in its vector diagram, (i).

fall on the spectrum origin. As can be easily seen, *any* $(k_1,\ldots,k_m)$ impulse in the spectrum convolution can be made singular by sliding the vector sum $\Sigma_{i=1}^{m} k_i \mathbf{f}_i$ to the spectrum origin, namely: by appropriately modifying the vectors $\mathbf{f}_1,\ldots,\mathbf{f}_m$ (i.e., the frequencies and angles of the superposed layers). When the $(k_1,\ldots,k_m)$ impulse is located exactly on the spectrum origin we say that the corresponding $(k_1,\ldots,k_m)$ moiré has become singular.

2.4 *Impulse Clusters in the Spectrum Convolution; Moiré Extraction*

Figure 3(f) shows the spectrum of the superposition of two onefold periodic images, namely: the convolution of their original nail bed spectra. As we can see, the spectrum convolution consists of a ''forest'' of impulses (with real or complex amplitudes, depending on the symmetry properties in the image domain). It has been shown[8] that the occurence of a moiré phenomenon in the image superposition is associated with the appearance of impulse combs or clusters in the spectrum, as in Fig. 3(f). In particular, it has been shown there that the main cluster, the infinite impulse cluster which is centered on the spectrum origin and whose fundamental impulse is $(k_1,\ldots,k_m)$, represents in the spectrum the $(k_1,\ldots,k_m)$-moiré effect generated in the superposition. And indeed, by extracting this impulse cluster from the spectrum and taking its inverse Fourier transform, one obtains, back in the image domain, the isolated contribution of the moiré in question to the superposition, i.e., the moiré intensity profile. Note that when a moiré effect becomes singular each of its impulse clusters collapses into a single location in the spectrum, and all the cluster's impulses fuse down into a single impulse, that we call a *compound impulse*. The amplitude of a compound impulse equals the sum of the amplitudes of its original impulses (see Sec. 9.3 in Ref. 9).

3 Rosettes in Singular States

Let us start by exploring the microstructure in moiré-free singular cases, where the superposition looks uniform and no macromoirés are visible. Since in these cases the only structure which appears in the image domain is the microstructure, it is clear that their spectra only represent the microstructure. Such cases will serve us as a starting point for studying the spectral representation of the microstructure. The microstructure in the case of *stable* moiré-free superpositions will be discussed later, in Sec. 4.2.

As we have seen, each impulse in the spectrum of a singular state is, in fact, a compound impulse representing a full cluster of impulses which has collapsed into a single location. According to the algebraic structure of the compound spectrum, we can distinguish here between two types of singular cases: singular cases in which the spectrum support is a discrete lattice and the layer superposition is periodic; and singular cases in which the spectrum support is a dense module and the layer superposition yields an almost-periodic image. (An explanation of these terms, as well as the conditions for a superposition to be periodic or almost periodic, can be found in Ref. 9; see Proposition 3 on p. 127 there. As an illustration to the term ''dense,'' one may think of the set $\mathbb{Q}$ of all rational numbers, which is everywhere dense in $\mathbb{R}$, and yet only countably infinite and nowhere continuous.) We will illustrate the first case by the singular (1, 2, −2, −1) moiré between two identical screens with angle difference of $\alpha=\arctan\frac{3}{4}\approx 36.87°$, and the second case by the singular moiré between three identical screens with equal angle differences of 30° (i.e., the conventional singular screen combination traditionally used in color printing).

3.1 *Rosettes in Periodic Singular States*

Let us consider the microstructure which occurs in a periodic singular case, such as the (1, 2, −2, −1)-singular superposition of two screens (Fig. 5). As we can see, the superposition in this case is periodic, and the rosettes are ordered in a perfectly repetitive pattern. And indeed, the spectrum of this superposition is a compound nail bed [Fig. 5(a)], where each impulse represents a collapsed cluster. Since the only structure which appears here in the superposition is the microstructure, it is clear that this nail bed represents the periodic microstructure of the superposition. And, indeed, the two fundamental (compound) impulses of this nail bed (whose frequency vectors **g** and **h** are a basis of the lattice of clusters in the spectrum support) determine the frequency and the direction of the microstructure in the image domain. In our example of the (1, 2, −2, −1)-singular state the frequency of the microstructure is, by the Pythagoras theorem, $g=f_1/\sqrt{5}$ [see Fig. 5(a)], and hence its period is $\sqrt{5}\approx 2.236$ times larger than the screen period; its orientation is $\varphi=\arctan(2)\approx 63.435°$ with respect to $\mathbf{f}_1$ (see note a in Notes section).

3.2 *Rosettes in Almost-Periodic Singular States*

Let us now consider the microstructure obtained in an almost-periodic singular case, such as the conventional singular three-screen superposition (see Fig. 6). Obviously, in this case there is no rosette periodicity in the superposed image. Rather, we can detect here in the image domain ''almost'' periodicities, and the rosette forms are only almost repetitive. This explains the fuzzy and elusive look of the microstructure in this case: looking at any location in the superposition, the eye is tempted at first to believe that the rosette structures are repetitive; but after a more careful examination it realizes that this repetition is just an illusion.

For example, let us look carefully at the almost-periodic rosette pattern of Fig. 6(b), in which the three screens are superposed in phase (i.e., they have a common dot at the origin). Clearly, apart from the origin, nowhere else in the superposition does there occur again a precise three-screens dot match (otherwise the superposition would be periodic). But at an infinite number of locations in the superposition there occurs an almost three-screens dot match [this may be better perceived in the magnification shown in Fig. 13(c)]. The farther we go from the origin, the better the almost matches that we can find. This is, indeed, a characteristic property of almost-periodic functions.

In the spectral domain, the spectrum of an almost-periodic singular case is no longer a compound nail bed whose support is a discrete lattice, but rather a forest of compound impulses (each of which representing a collapsed cluster), whose support is a dense module [see Fig. 6(a)]. And again, since the only structure which appears here in the superposition is the microstructure, it is clear

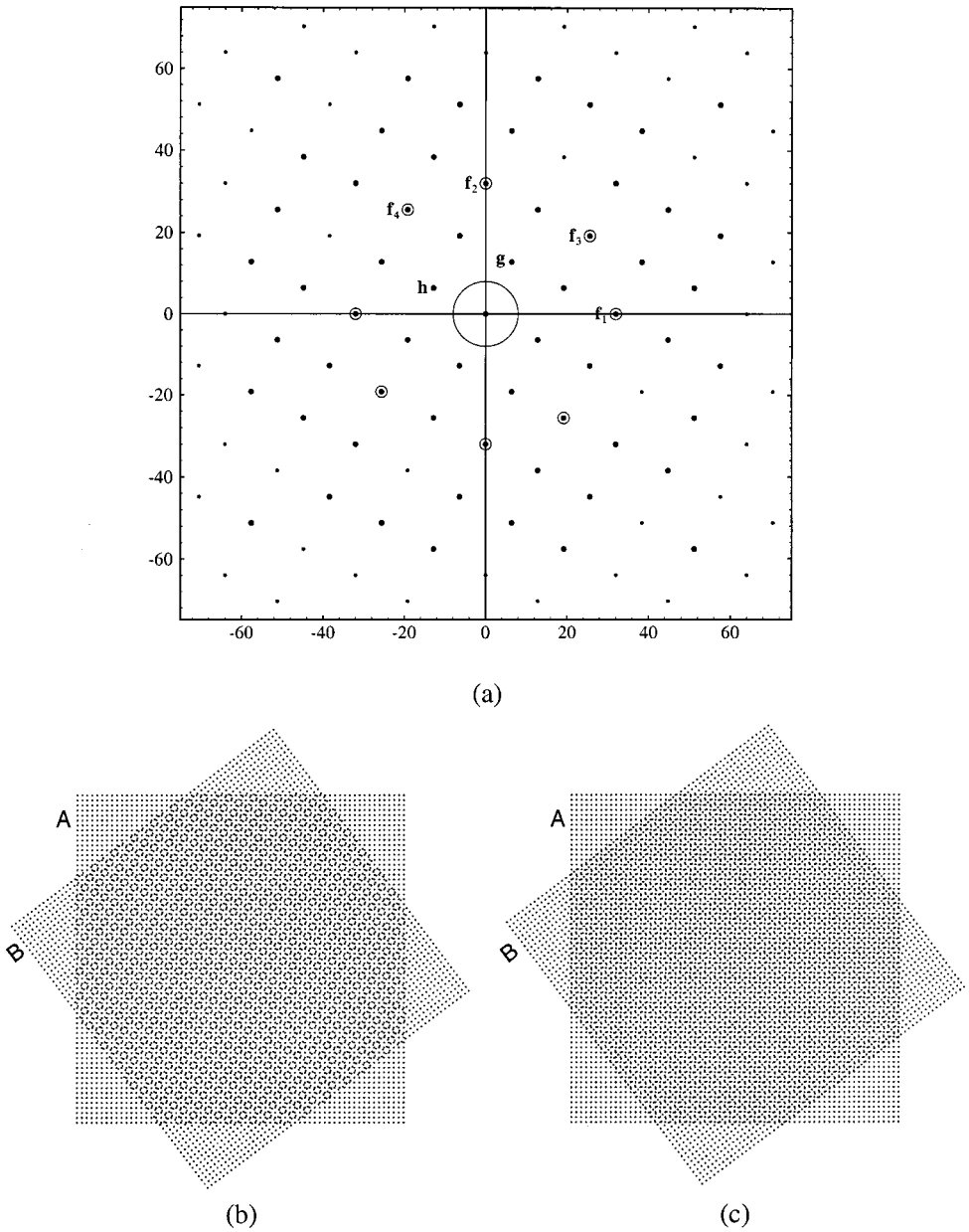

Fig. 5 The singular (1,2,−2,−1)-superposition of two identical screens with angle difference of $\alpha = \arctan\frac{3}{4} \approx 36.87°$. (a): The spectrum support; $\mathbf{f}_1, \ldots, \mathbf{f}_4$ are the fundamental frequency vectors of the two original screens, and **g** and **h** are the fundamental compound impulses of the microstructure. The circle in the center of the spectrum represents the visibility circle. (b), (c): The screen superposition in the image domain: in-phase superposition in (b), and counter-phase superposition in (c). Note the uniformity of the microstructure, and the difference between the rosette shapes in (b) and (c).

that this ''compound module'' represents the almost-periodic microstructure of the superposition.

3.3 *Influence of Layer Shifts on Rosettes in Singular States*

It has already been shown[10] that shifts in the individual superposed layers may cause, depending on the case, either a global shift (a rigid motion) of the superposition as a whole, or a real modification in the microstructure of the superposition. Figures 5(b) and 5(c) and 6(b) and 6(c) illustrate the microstructure modifications which occur due to such shifts in different singular screen superpositions; Fig. 5 shows a case in which the screen superposition is periodic, and Fig. 6 shows a case in which the superposition is almost periodic. It is important to note that when the superposition is periodic, as in Fig. 5, the microstructure modifications that are caused by the shifts do not influence this periodicity or its orientation, but only the internal structure within each period (namely, the rosette shapes).

If we examine the forms of the rosettes which are generated as the phase of the original layers is being modified, we find two extreme types of rosettes, as well as all the possible intermediate types which occur between them. One extreme type occurs when the original layers are su-

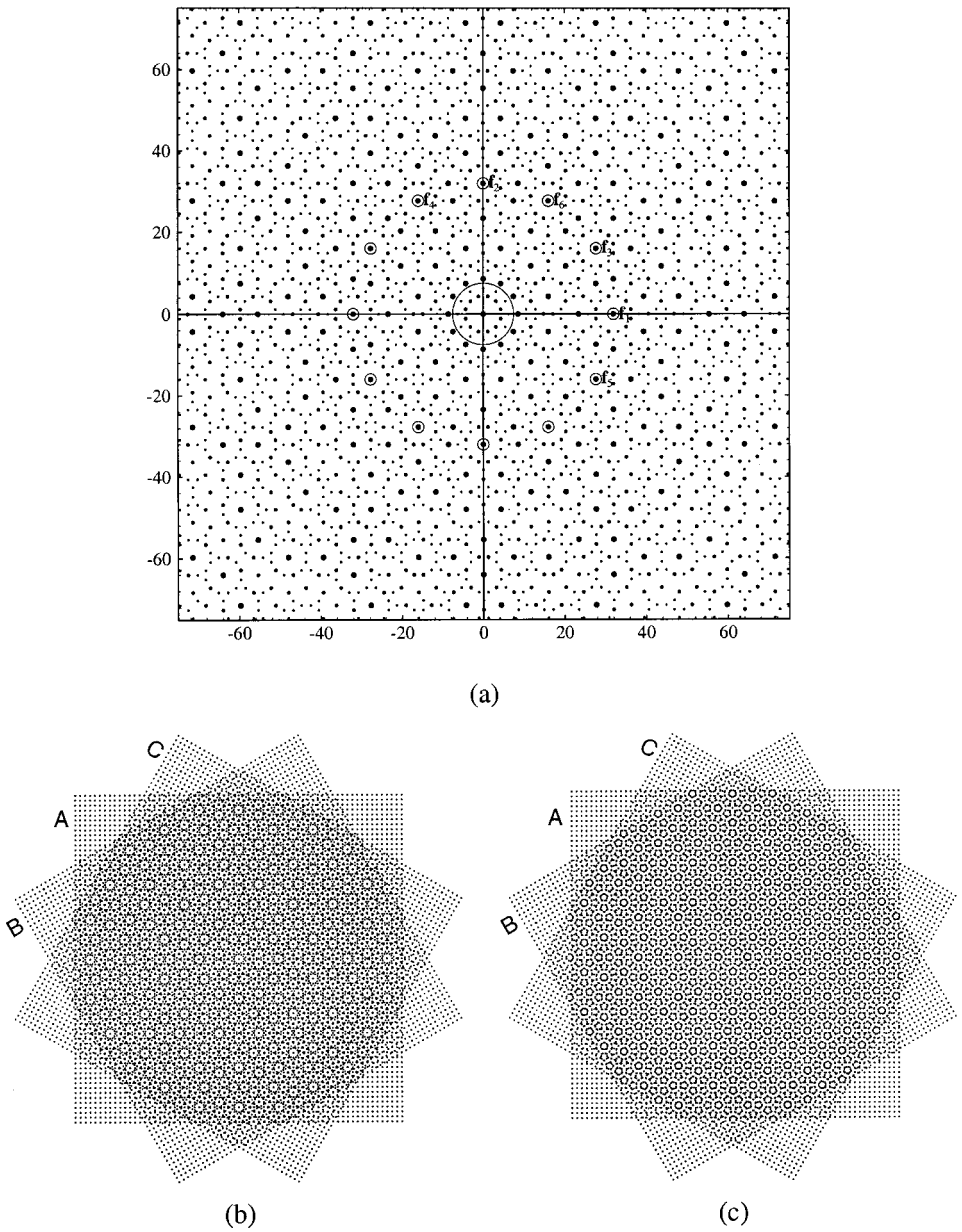

Fig. 6 The singular superposition of three identical screens at equal angle differences of 30°. (a): The spectrum support (showing only impulses up to order three). (b), (c): The screen superposition in the image domain: in-phase superposition in (b), and counter-phase superposition in (c). Note the uniformity of the microstructure, and the difference between the rosette shapes in (b) and (c).

perposed ''in phase,'' i.e., when each layer has a black element (dot or line) centered on the origin; and the other extreme type occurs when the original layers are superposed in counter phase. A gradual transition between these extreme rosette forms occurs in the intermediate phase positions.

These two extreme rosette forms are illustrated in Figs. 5(b) and 5(c) for the case of the periodic (1, 2, −2, −1)-singular moiré, and in Figs. 6(b) and 6(c) for the almost-periodic case of the classical three-screen superposition with identical frequencies and angle differences.

The precise rosette shapes and their variations due to lateral shifts in the superposed layers are characteristic properties (like ''fingerprints'') of each particular singular state. Most famous are the rosette forms obtained in the classical superposition of three identical screens with equal angle differences; these rosette forms are well known in the printing industry and they have been widely described in literature (Ref. 1, pp. 339–341; Ref. 4, pp. 57–59; Ref. 5). As illustrated in Fig. 6(b), when the three screens are superposed in phase, i.e., with a black dot centered on the origin, a perfect match of one screen dot from each layer occurs at the origin. This generates at the origin the form of a ''dot-centered'' rosette. Due to the almost periodicity, ''almost-perfect'' copies of this dot-centered rosette can be found at any distance from the origin, thus generating a uniform microstructure with almost-dot-centered rosettes

throughout. However, when the screens are superposed in counter phase, a ''clear-centered'' rosette pattern is generated [see Fig. 6(c)]. It should be emphasized, however, that the rosette shapes obtained in other singular states may be completely different; and as we can see in the case of the singular (1, 2, −2, −1) moirés [Figs. 5(b) and 5(c)], even the terms ''dot-centered'' and ''clear-centered'' may no longer be appropriate for the in-phase and counter-phase rosettes.

It is interesting to ask now how do such variations in the rosette shapes due to layer shifts in the superposition reflect in the spectrum of the singular case? And, furthermore, why in some singular cases the difference between the two extreme rosette types is very significant, while in other singular cases the difference is hardly distinguishable? As we have seen in Sec. 2.4, the amplitude of each impulse in the spectrum of a singular superposition (i.e., the amplitude of each compound impulse) is the sum of the amplitudes of all the individual impulses which collapsed onto the same location. On the other hand, according to the shift theorem (Ref. 6, p. 104) a shift in any of the superposed layers modifies the complex amplitudes of the impulses in its own spectrum. The answer to the above questions is found, therefore, in the way in which variations in the complex amplitudes of the individual impulses within each collapsed cluster influence the summed-up complex amplitude of the resulting compound impulse: in some cases the variations in the summed-up amplitudes may be significant, while in other cases they may be cancelled out. The variations in the complex amplitudes of the compound impulses due to the shifts in the superposed layers reflect, therefore, the variations in the rosette shapes as a function of the shifts in the individual layers.

4 Microstructure in Nonsingular States

After having explored the microstructure behavior in singular superpositions, we arrive now to the case of nonsingular states. We will first discuss the microstructure slightly off a singular state, where a macromoiré is clearly visible, and then we will proceed to the case of stable moiré-free superpositions, away from any visible macromoiré effect.

4.1 *Microstructure Slightly off a Singular State*

As we already know, when we slightly move away from the singular state of a given moiré, this moiré becomes visible in the superposition in the form of a moiré effect with a large, visible period. Looking now at this superposition through a magnifying glass, we discover that, in fact, the visible macrostructures are constructed from the microstructures of the superposition. The key point in the relationship between macro- and microstructures in the superposition can be stated as follows:

Proposition 1: When the microstructures of the superposition are similar and uniformly distributed throughout the superposed image, the resulting superposition looks from a distance uniform and smooth, and no moiré is visible (see, for instance, Figs. 5 and 6). However, if different types of rosettes are generated in alternate areas of the superposed image, the eye observes a different gray level in each of these areas (due to the different surface-covering rates of the dots in the different rosette types), and a macromoiré becomes visible [see Figs. 7 and 8, or Fig. 4(h) and its magnification in Fig. 1(a)]. This is, in fact, the microscopic interpretation of the macroscopic moiré patterns. ■

However, this is not yet all. Looking carefully at the microstructure of any given macromoiré, we discover that the relationship between the micro- and the macrostructures is even deeper than what is stated in Proposition 1. In fact, we have:

Proposition 2: The microstructure alternations which make up a macromoiré are, to a very close approximation, nothing else but the microstructure forms which are obtained at the singular state of that macromoiré by all possible phase shifts. The two extreme in-phase and ''counter-phase'' microstructures (e.g., the dot-centered and the ''clear-centered'' rosettes in the case of the classical three-screen superposition) generate the two extreme intensity levels of the visible macromoiré (its brightest and darkest areas), and the intermediate forms between them generate all the in-between intensity levels of the macromoiré (see note b in Notes section). ■

This can be clearly illustrated for the (1,2,−2,−1) moiré by comparing Fig. 7(b) with Figs. 5(b) and 5(c), and for the classical three-screen superposition by comparing Fig. 8(b) with Figs. 6(b) and 6(c).

It should be emphasized, however, that Proposition 2 is only a close approximation. The reason is that as the angles or the frequencies are slightly modified in order to move our macromoiré slightly away from its singular state, the microstructures are also slightly modified. However, the closer the macromoiré is to its singular state, the better the approximation provided by Proposition 2.

4.2 *Microstructure in Stable Moiré-free Superpositions*

Let us now consider the microstructures which occur in stable moiré-free superpositions, such as the superposition of two identical screens with an angle difference of 30° (see Fig. 9). Just like singular moiré-free states (Sec. 3), stable moiré-free superpositions have no visible macromoirés, and they show a uniform-looking microstructure. However, this is also where the similarity between these two types of moiré-free superpositions ends. Stable moiré-free cases are not singular superpositions, and, therefore, their tolerance to layer rotations, scalings, and shifts is significantly higher. This means that in all the neighboring layer combinations which are still included within the tolerance limits (i.e., within a certain reasonable interval of angles and frequencies around the given superposition) no macromoirés are visible, and hence, in terms of Proposition 1, no significant microstructure variations occur in the superposition. The microstructure of such cases seems to be ''uniformly disordered,'' meaning that it consists of a uniform but nonperiodic blend of various types of rosettes. Moreover, although this microstructure varies when the superposed layers are rotated or scaled within the tolerance limits, its overall look remains unchanged. In particular, no visible rosette-type changes occur in such cases owing to layer shifts; this can be clearly seen in Figs. 9(b) and 9(c), in contrast to Figs. 5 and 6 where rosette-type changes owing to layer shifts

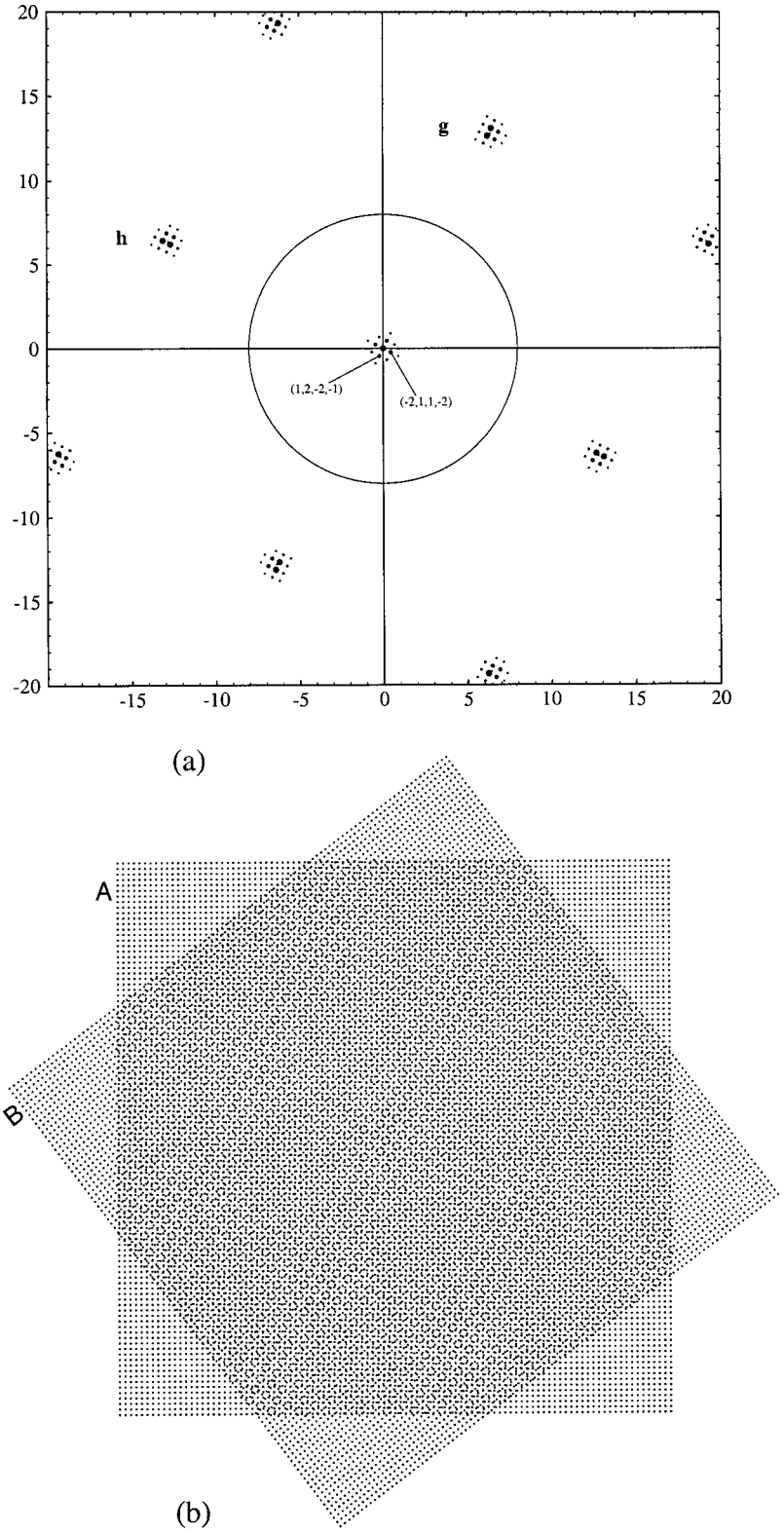

Fig. 7 The (1,2,−2,−1) moiré of Fig. 5 slightly off its singular state; (a) shows the corresponding spectrum (only impulses up to the fourth harmonic are shown). The scale in the spectral domain was changed for the sake of clarity.

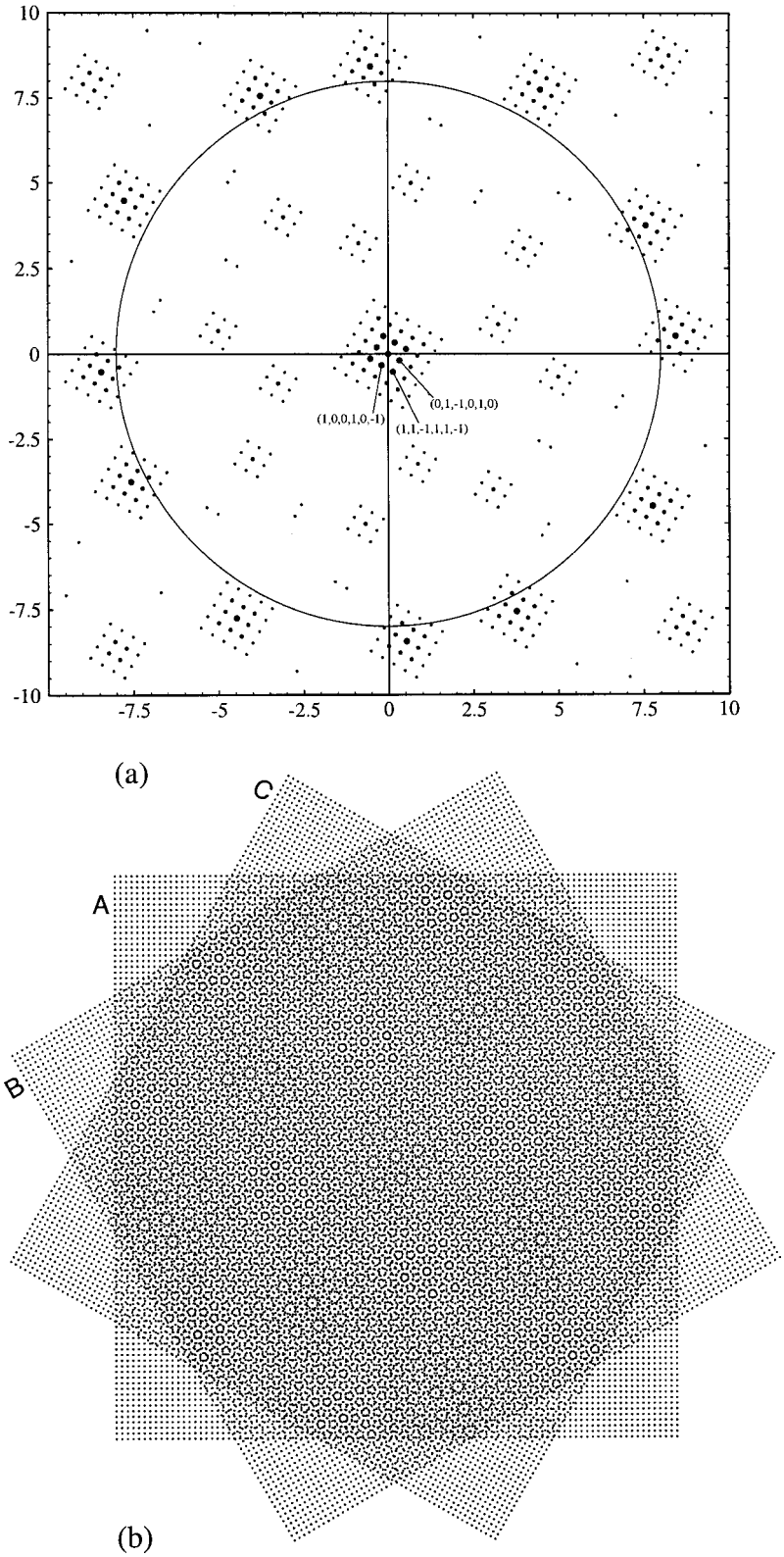

Fig. 8 The classical three-screen moiré of Fig. 6 slightly off its singular state; (a) shows an enlarged view of the central part of the corresponding spectrum (only impulses up to order three are shown). The scale in the spectral domain was changed for the sake of clarity.

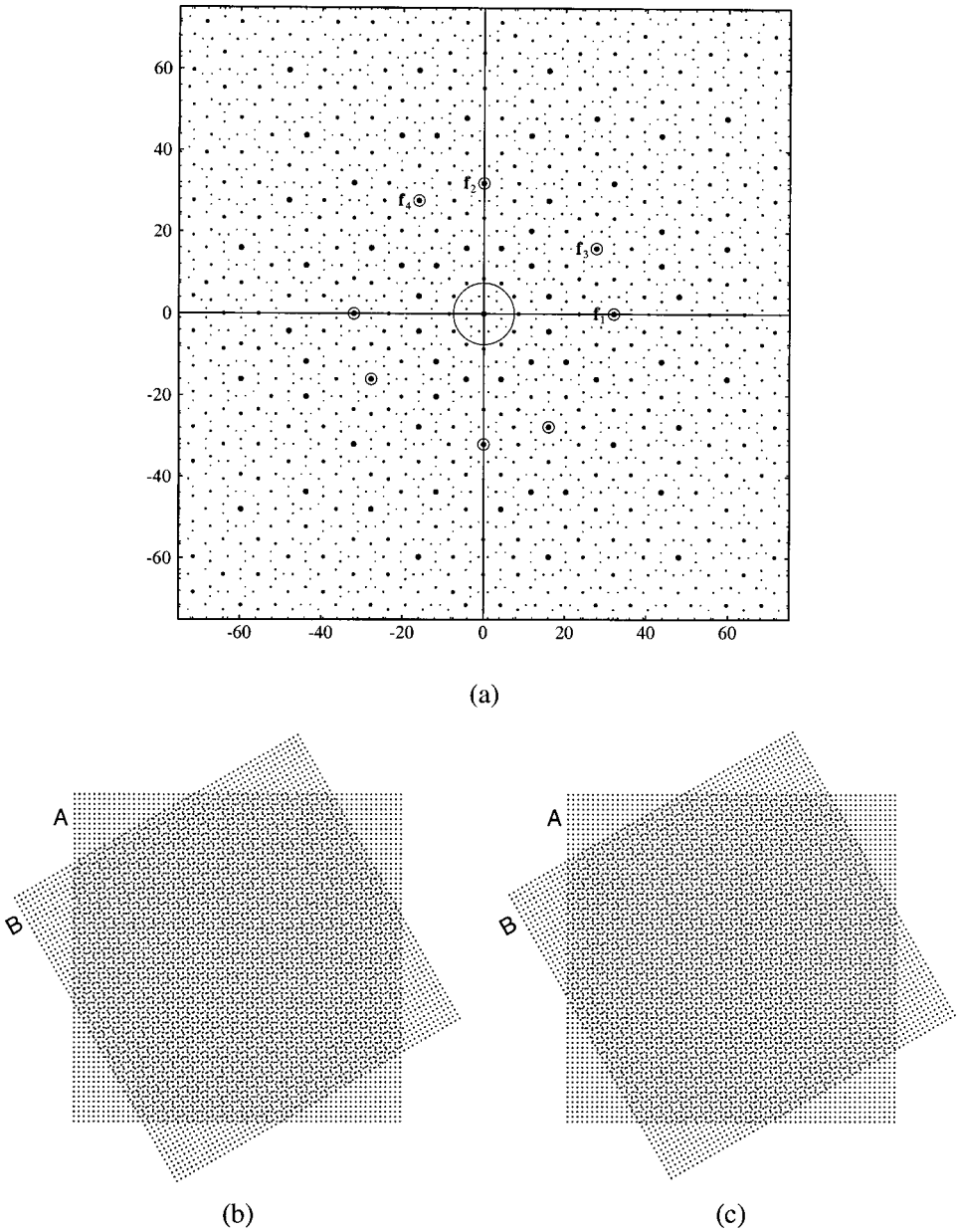

Fig. 9 The stable moiré-free superposition of two identical screens with angle difference of $\alpha = 30°$. (a): The spectrum support (showing only impulses up to order five). (b), (c): The screen superposition in the image domain: in-phase superposition in (b), and counter-phase superposition in (c). Note the uniformity of the microstructure; however, unlike in Fig. 6, no visible differences exist between the rosette shapes in (b) and (c). The spectrum support (a) is the same as in the singular three-screen superposition of Fig. 6(a), but this time it consists of simple impulses and not of compound impulses (collapsed clusters).

are clearly visible. This curious difference in the microstructure behavior between singular and nonsingular moiré-free cases will be fully elucidated in the sections which follow.

The difference between singular and stable moiré-free superpositions is also remarkable in the spectral domain: while in singular states each impulse in the spectrum is, in fact, a compound impulse representing a full cluster of impulses which have collapsed into a single location, in stable moiré-free cases each impulse in the spectrum has its own distinct location, and different impulses do not fall together on the same point. This fact provides, indeed, the spectral domain interpretation of the microstructure invariance under layer shifts in stable moiré-free superpositions (see last paragraph in Sec. 3.3).

An example of a three-screen stable moiré-free superposition is shown in Ref. 11, Fig. 19, or in Ref. 14, p. 76. Its microstructure has, again, the same basic properties: it looks uniformly disordered, and it does not present substan-

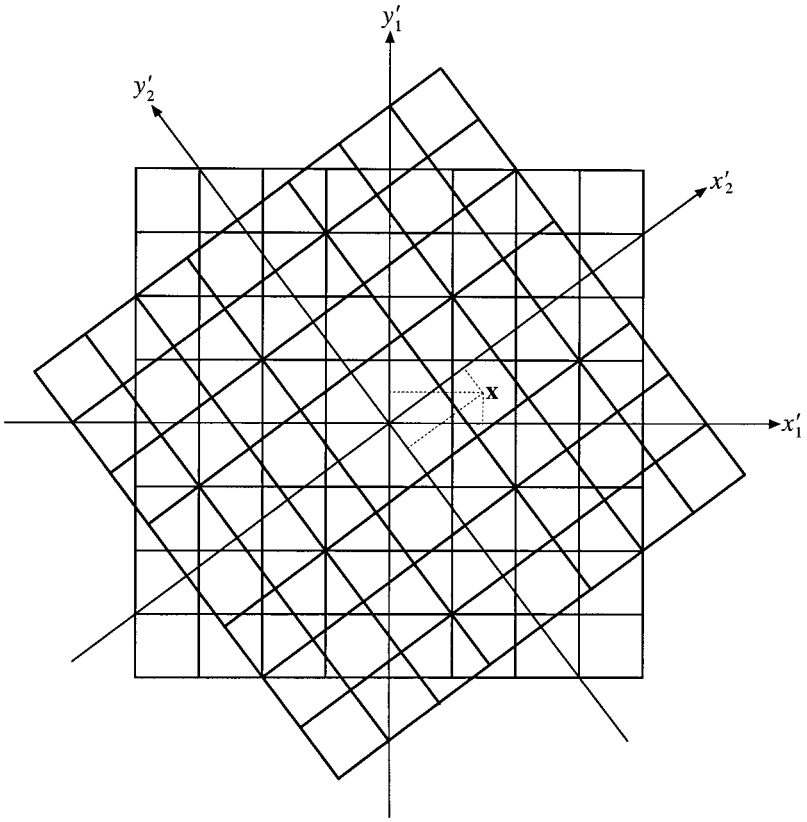

Fig. 10 A magnified view of the superposition of two identical square grids with an angle difference of $\alpha = \arctan\frac{3}{4} \approx 36.87°$ (compare with Fig. 5). The period coordinates of point **x** in the superposition are $\xi_1 = \frac{3}{2}$, $\xi_2 = \frac{1}{2}$, $\xi_3 = \frac{3}{2}$, and $\xi_4 = -\frac{1}{2}$. For the sake of simplicity we chose the x'_1, y'_1 coordinates to coincide with the x and y axes of the x,y plane.

tial changes under layer shifts (as well as under layer rotations and scalings within the specified tolerance limits).

5 Algebraic Formalization

Having described the various interesting phenomena related to the microstructure of the superposition, we are ready now to introduce an algebraic formalization that will help us to elucidate these phenomena.

Let us start with a simple example to illustrate our line of thought and to motivate our algebraic approach.

Example 1: Consider the superposition of two identical square grids (or dot screens) with an angle difference of $\alpha = \arctan\frac{3}{4} \approx 36.87°$, as in Fig. 5 (see the magnified view in Fig. 10). Clearly, each point **x** in the x,y plane (i.e., in the superposition) can be expressed in terms of the coordinate system x'_1, y'_1 of the first grid, as well as in terms of the coordinate system x'_2, y'_2 of the second grid. However, we will find it advantageous to express point **x** in the coordinate system of each of these square grids in terms of the grid's own period T_i. Hence, for each square grid i in the superposition ($i = 1,2$) we define the *period-coordinates* ξ_{2i-1} and ξ_{2i} at the point **x** as the coordinates of point **x** in the coordinate system x'_i, y'_i of that grid, expressed in terms of periods T_i. Table 1 gives the period coordinates of the two grids of Fig. 10 at various points $\mathbf{x} = (x,y)$ in the superposition, along with a verbal description of the microstructure of the superposition at these points.

Table 1 The period coordinates of the two grids in Fig. 10 at various points $\mathbf{x} = (x,y)$.

(x,y)	$(\xi_1,\xi_2,\xi_3,\xi_4)$	Microstructure at (x,y):
(0,0)	(0,0,0,0)	Center of a dot-centered rosette
$(\frac{3}{2}T, \frac{1}{2}T)$	$(\frac{3}{2}, \frac{1}{2}, \frac{3}{2}, -\frac{1}{2})$	Center of a clear-centered rosette
$(\frac{1}{2}T, T)$	$(\frac{1}{2}, 1, 1, \frac{1}{2})$	...
$(T, 2T)$	(1,2,2,1)	Center of a dot-centered rosette

Note that the period-coordinates ξ_i should not be confused with the period-shifts ϕ_i (see Ref. 10). The period-shifts ϕ_i have been introduced for expressing *shifts* of periodic layers in terms of number of periods. The period-coordinates ξ_i, for their part, express in terms of number of periods the coordinates of any point **x** within a static superposition. Note that when a layer shift occurs the origin and the coordinate system of the shifted layers are displaced within the x,y plane, so that the period-coordinate ξ_i of any point **x** in the superposition is decremented by the period-shift ϕ_i which corresponds to that layer shift. For instance, assume that the second grid of our example is shifted by half a period in each of its two main directions; this layer shift is expressed by the period shifts $(\phi_1, \phi_2, \phi_3, \phi_4)$

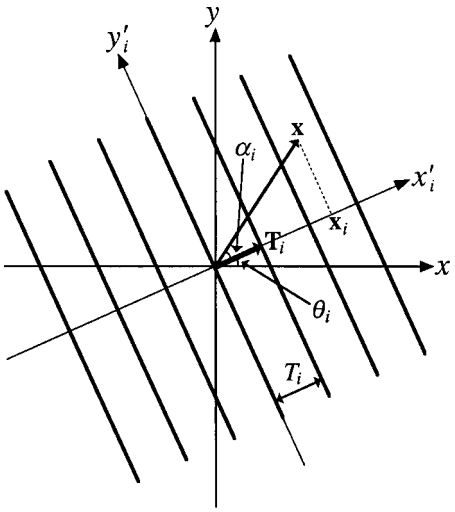

Fig. 11 A schematic view of layer i in the superposition, showing $\mathbf{x}_i$, the projection of point $\mathbf{x}=(x,y)$ on axis x'_i. θ_i is the orientation of axis x'_i, and α_i is the angle formed between the direction of point $\mathbf{x}$ and axis x'_i. The coordinates of point $\mathbf{x}_i$ are (x_i,y_i) in terms of the x,y plane, and $(x'_i,0)$ in terms of the x'_i,y'_i coordinates of the ith layer. The period coordinate of point $\mathbf{x}$ with respect to axis x'_i is $\xi_i=\frac{5}{2}$.

$=(0,0,\frac{1}{2},\frac{1}{2})$. Therefore, at any point $\mathbf{x}$ in the superposition the new period coordinates after the shift are given by

$$(\xi_1,\xi_2,\xi_3,\xi_4)_{\text{new}}=(\xi_1,\xi_2,\xi_3,\xi_4)_{\text{old}}-(\phi_1,\phi_2,\phi_3,\phi_4).$$

By analogy with the phase terminology we call the vector $(\xi_1,\xi_2,\xi_3,\xi_4)$ the *period-coordinate vector of the superposition* at the point (x,y). As we can see, the period-coordinate vector $(\xi_1,\xi_2,\xi_3,\xi_4)$ at any point (x,y) is strongly related to the local microstructure of the superposition at that point. For example, whenever $(\xi_1,\xi_2,\xi_3,\xi_4)$ is purely integer, i.e., $(\xi_1,\xi_2,\xi_3,\xi_4)\in\mathbb{Z}^4$, the superposition at (x,y) contains a meeting point of full periods in all layers, which means that point (x,y) is the center of a dot-centered rosette. Similarly, whenever the ξ_i values are all half integers (i.e., $\xi_i=k_i+\frac{1}{2}$, $k_i\in\mathbb{Z}$), the point (x,y) in the superposition is the center of a clear-centered rosette.

Now, if we run throughout all the points $(x,y)\in\mathbb{R}^2$ (i.e., throughout the whole superposition), which parts of $\mathbb{R}^4$ will be occupied by the corresponding points $(\xi_1,\xi_2,\xi_3,\xi_4)$? It is clear that $\mathbb{R}^4$ will not be completely filled; for instance, in the present superposition (see Fig. 10) the point $(0, 0, -\frac{1}{2}, -\frac{1}{2})$ cannot be obtained—it can only be obtained when the second layer is shifted by half a period in each of its two main directions. In order to investigate this (and other) questions, we find it useful to define a transformation $\Xi:\mathbb{R}^2\to\mathbb{R}^4$, which gives for any point (x,y) in the superposition plane its corresponding point $(\xi_1,\xi_2,\xi_3,\xi_4)$ in $\mathbb{R}^4$. And, indeed, we will see below that the investigation of this transformation and of its properties will shed a new light onto the microstructure and the phase relationships of the layer superposition. ■

Having explained the motivation for the proposed algebraic formalization, we are ready now to go back to the general case and to introduce our new formal approach.

Let $p_1(\mathbf{x}),\ldots,p_m(\mathbf{x})$ be m onefold periodic functions (gratings) given in their initial phase, so that their origins coincide with the origin of the x,y plane, and let $p(\mathbf{x})=p_1(\mathbf{x})\cdot\ldots\cdot p_m(\mathbf{x})$ be their superposition. (Note that a pair of onefold periodic functions may represent in the superposition one twofold periodic function, such as a dot screen.) We remember that the main periodicity direction of the ith grating is the direction θ_i along which the grating has the smallest period>0. Now, let $\mathbf{x}$ be a point in the x,y superposition plane. For each grating i of the superposition we define the period-coordinate ξ_i at point $\mathbf{x}$ as the number (integer or not) of periods $\mathbf{T}_i$ between the grating origin and $\mathbf{x}_i$, the projection of $\mathbf{x}$ on the axis defining the main periodicity direction of grating i. In other words, ξ_i is the 1D coordinate of the point $\mathbf{x}$ on this axis, expressed in period units (see Fig. 11). If α_i is the angle formed between the direction of point $\mathbf{x}$ and the main periodicity direction of grating i we have, therefore

$$\xi_i=\frac{|\mathbf{x}|\cos\alpha_i}{|\mathbf{T}_i|}=\frac{|\mathbf{x}_i|}{|\mathbf{T}_i|}$$

and hence: $\mathbf{x}_i=\xi_i\mathbf{T}_i$. Remembering that $\mathbf{T}_i\cdot\mathbf{T}_i^{-1}=1$ (see Ref. 10, pp. 979 and 987) we multiply both sides (in the sense of scalar product) by $\mathbf{T}_i^{-1}$, and hence we obtain $\mathbf{x}_i\cdot\mathbf{T}_i^{-1}=\xi_i$. Using $\mathbf{f}_i=\mathbf{T}_i^{-1}$ [see Ref. 10, Eq. (A6)], where $\mathbf{f}_i$ is the frequency vector of the onefold periodic function $p_i(\mathbf{x})$, we obtain

$$\xi_i=\mathbf{f}_i\cdot\mathbf{x}_i. \tag{7}$$

Now, we remember that the scalar product (i.e., inner product) $\mathbf{v}\cdot\mathbf{w}$ can be understood as a number which gives the product of the length of vector $\mathbf{v}$ by the length of the projection of vector $\mathbf{w}$ on the direction of $\mathbf{v}$ (or vice versa)[12]

$$\mathbf{v}\cdot\mathbf{w}=|\mathbf{v}||\text{proj}(\mathbf{w})_{\mathbf{v}}|.$$

This means that for any point $\mathbf{x}$ in the x,y plane we have

$$\mathbf{f}_i\cdot\mathbf{x}=\mathbf{f}_i\cdot\mathbf{x}_i, \tag{8}$$

where $\mathbf{x}_i$ is the projection of $\mathbf{x}$ on the direction of $\mathbf{f}_i$. Therefore Eq. (7) can be reformulated as

$$\xi_i=\mathbf{f}_i\cdot\mathbf{x}. \tag{9}$$

The period-coordinate ξ_i can be also expressed in the form $\xi_i=g_i(x,y)$ as a function of the plane coordinates x,y: Let $\mathbf{x}=(x,y)$ be a point in the plane, and let the x'_i axis through the origin represent the main periodicity direction θ_i of the ith grating. We also denote by y'_i the axis perpendicular to x'_i through the origin (see Fig. 11). The coordinates of point $\mathbf{x}$ in terms of the rotated axes x'_i, y'_i are

$$x'_i=x\cos\theta_i+y\sin\theta_i$$

$$y'_i = -x \sin\theta_i + y \cos\theta_i$$

and, therefore, the projection of the point $\mathbf{x}$ on the x'_i axis is given in terms of these rotated coordinates by: $\mathbf{x}_i = (x'_i, 0)$. This means that ξ_i is explicitly given in the form $\xi_i = g_i(x,y)$ by

$$\xi_i = g_i(x,y) = \frac{x'_i}{T_i} = x\frac{\cos\theta_i}{T_i} + y\frac{\sin\theta_i}{T_i}, \tag{10}$$

where $x'_i = |\mathbf{x}_i|$ and $T_i = |\mathbf{T}_i|$.

As we can see, for each layer i of the superposition, the period-coordinate ξ_i is uniquely defined at any point $\mathbf{x} = (x,y)$ of the plane. Therefore, we may define a transformation $\Xi: \mathbb{R}^2 \to \mathbb{R}^m$, called the *period-coordinate function*, which gives for any point $\mathbf{x} = (x,y)$ in the plane the period-coordinate ξ_i of this point in each of the m superposed onefold periodic layers

$$\Xi(x,y) = (\xi_i, \ldots, \xi_m). \tag{11}$$

In other words, this transformation gives for any point $\mathbf{x} = (x,y)$ in the superposition plane its coordinates in the main direction of each of the m layers, in terms of each layer's period. Since each of the functions $\xi_i = g_i(x,y)$ is linear, i.e., $\xi_i = a_i x + b_i y$ [see Eq. (10)] it follows that $(\xi_1, \ldots, \xi_m)$ too is linear in x and y, so that Ξ is a linear transformation. Therefore, the image of Ξ is a linear subspace within $\mathbb{R}^m$ whose dimension is 2, namely: Ξ maps the x,y superposition plane into a plane $\mathrm{Im}\,\Xi$ within $\mathbb{R}^m$ which passes through the origin. Note that the subspace $\mathrm{Im}(\Xi)$ may have a lower dimension than 2 if the transformation Ξ is degenerate; for example, if all the m superposed gratings have the same orientation, so that $\xi_2, \ldots, \xi_m$ are constant multiples of ξ_1, then all the vectors $(\xi_1, \ldots, \xi_m) \in \mathbb{R}^m$ are collinear and $\dim \mathrm{Im}(\Xi) = 1$. Such degenerate cases will generally be ignored in the discussions which follow (see note c in Notes section).

Let us now consider the plane $\mathrm{Im}(\Xi)$ which is defined by the transformation (Ξ) within $\mathbb{R}^m$. Points $(\xi_1, \ldots, \xi_m)$ in $\mathrm{Im}(\Xi)$ which are only composed of integer values have a special significance, since they indicate that the corresponding point (x,y) in the superposition is located on a junction of full periods from the origin in all of the superposed layers. Since we have assumed that the onefold periodic functions $p_1(\mathbf{x}), \ldots, p_m(\mathbf{x})$ are given in their initial phase, we know that the plane $\mathrm{Im}(\Xi)$ contains at least the point (0,...,0); but does it contain any other integer point $(k_1, \ldots, k_m)$? Clearly, if $\mathrm{Im}(\Xi)$ contains an integer point $(k_1, \ldots, k_m) \neq (0,...,0)$, then it also contains the whole 1D lattice L defined by the integer multiples $n(k_1, \ldots, k_m)$, and the superposition is onefold periodic; and if $\mathrm{Im}(\Xi)$ contains two integer points $(k_1^{(1)}, \ldots, k_m^{(1)}) \neq (0,...,0)$ and $(k_1^{(2)}, \ldots, k_m^{(2)}) \neq (0,...,0)$ which are not on the same line through the origin, then it contains the whole 2D lattice L defined by their integer linear combinations: $i(k_1^{(1)}, \ldots, k_m^{(1)}) + j(k_1^{(2)}, \ldots, k_m^{(2)})$, and the superposition is twofold periodic. Depending on the plane inclinations within the space $\mathbb{R}^m$ the lattice $L \subset \mathrm{Im}(\Xi)$ may have rank $= 2$ (in the case of $m = 3$ this happens, for instance, if the plane $\mathrm{Im}(\Xi)$ contains both the x and y axes of $\mathbb{R}^3$); rank $= 1$ (e.g., if the plane only contains the x axis of $\mathbb{R}^3$ but forms an irrational angle with the y and z axes); or rank $= 0$ [if the only integral point in the plane is the origin (0,...,0)].

Example 2: Consider the superposition of two identical periodic square grids (or dot screens) which are rotated by angles 0 and α, respectively. The transformation Ξ is given in this case by

$$\Xi\begin{pmatrix} x \\ y \end{pmatrix} = \begin{pmatrix} \xi_1 \\ \xi_2 \\ \xi_3 \\ \xi_4 \end{pmatrix} = \frac{1}{T}\begin{pmatrix} x \\ y \\ x\cos\alpha + y\sin\alpha \\ -x\sin\alpha + y\cos\alpha \end{pmatrix} = \frac{1}{T}\begin{pmatrix} \begin{pmatrix} x \\ y \end{pmatrix} \\ M\begin{pmatrix} x \\ y \end{pmatrix} \end{pmatrix}, \tag{12}$$

where M is the 2×2 matrix which represents a rotation by angle α

$$M = \begin{pmatrix} \cos\alpha & \sin\alpha \\ -\sin\alpha & \cos\alpha \end{pmatrix}.$$

If $\tan\alpha$ is rational (as in the case of $\alpha = \arctan\frac{3}{4} \approx 36.87°$; see Example 1 and Fig. 5) then rank $L = 2$ and infinitely many points (x,y) in the superposition possess an integer vector $(\xi_1, \xi_2, \xi_3, \xi_4)$; the superposition in this case is twofold periodic. Note that since an integer vector $(\xi_1, \xi_2, \xi_3, \xi_4)$ represents in the superposition a meeting point of full periods, its corresponding point (x,y) in the superposition is a center of a dot-centered rosette. The effect of varying angle α (i.e., of rotating the second grid in the superposition) is a rotation of $\mathrm{Im}(\Xi)$ within its own plane in the space $\mathbb{R}^4$, about the origin.

If, however, $\tan\alpha$ is irrational, as in the case of $\alpha = 30°$ (see Fig. 9), then rank$L = 0$ and the plane $\mathrm{Im}(\Xi)$ does not contain any integer $(\xi_1, \xi_2, \xi_3, \xi_4)$ except for the origin (0,...,0). This means that at no point (x,y) in the superposition except for the origin is a precise dot-centered rosette formed. For similar reasons $\mathrm{Im}(\Xi)$ contains no points $(\xi_1, \xi_2, \xi_3, \xi_4)$ with half integers in all coordinates, meaning that at no point (x,y) in the superposition does there exist a meeting point of half periods, i.e., a clear-centered rosette. However, in the case of irrational $\tan\alpha$ the superposition contains infinitely many approximations of such rosettes (of either type) (see note d in Notes section); this can be clearly seen in Fig. 9. In such cases the screen superposition is not periodic but rather almost periodic; and indeed, as we have already seen, this type of microstructure is a characteristic property of almost-periodic functions. ■

Let us see now a few properties of the transformation Ξ that are related to lateral shifts of the superposed layers.

Proposition 3: Assume that the grating $p_i(\mathbf{x})$ in the superposition is laterally shifted by a vector $\mathbf{a}$; this shift can

be expressed, as we have seen in Ref. 10, by the period-shift $\phi_i = |\mathbf{a}_i|/\mathbf{T}_i|$, where $\mathbf{a}_i$ is the projection of $\mathbf{a}$ on the axis defining the direction of periodicity of $p_i(\mathbf{x})$, and $\mathbf{T}_i$ is the period of $p_i(\mathbf{x})$. Therefore, as a result of this shift, the period-coordinate ξ_i of any point (x,y) in the superposition is decremented by the period-shift ϕ_i. This means that the plane Im Ξ is shifted within $\mathbb{R}^m$ by ϕ_i along the axis of the ith dimension. ■

This result may be restated more formally as follows:

Let $\Xi(x,y)$ be the period-coordinate function which corresponds to the grating superposition $p_1(\mathbf{x})\cdot\ldots\cdot p_m(\mathbf{x})$. Suppose now that the gratings $p_1(\mathbf{x}),\ldots,p_m(\mathbf{x})$ undergo shifts of $\mathbf{a}_1,\ldots,\mathbf{a}_m$, respectively. Then, the period-coordinate function which corresponds to the superposition after the shift is given by

$$\Xi_A(x,y)=\Xi(x,y)-S_A(x,y)=(\xi_1,\ldots,\xi_m)-(\phi_1,\ldots,\phi_m), \tag{13}$$

where A denotes the multi-vector $(\mathbf{a}_1,\ldots,\mathbf{a}_m)$. Note that $\phi_i=\mathbf{f}_i\cdot\mathbf{a}_i$ (see Ref. 10, p. 979) and $\xi_i=\mathbf{f}_i\cdot\mathbf{x}_i$, where $\mathbf{x}_i$ is the projection of the point $\mathbf{x}$ on the direction of $\mathbf{f}_i$, the periodicity direction of the grating $p_i(\mathbf{x})$. The function $S_A:\mathbb{R}^2\rightarrow\mathbb{R}^m$ which defines the period shifts of the m gratings, $S_A(x,y)=(\phi_1,\ldots,\phi_m)$, is called the *period-shift function*; note that it returns the same constant vector for every point $\mathbf{x}$ in the superposition.

For example, if the second square grid (or dot screen) of Example 2 above is shifted by half a period in each of its two main directions, the transformation Ξ becomes

$$\Xi_A\begin{pmatrix}x\\y\end{pmatrix}=\begin{pmatrix}\xi_1\\\xi_2\\\xi_3\\\xi_4\end{pmatrix}=\frac{1}{T}\begin{bmatrix}\begin{pmatrix}x\\y\end{pmatrix}\\M\begin{pmatrix}x\\y\end{pmatrix}\end{bmatrix}-\begin{pmatrix}0\\0\\\frac{1}{2}\\\frac{1}{2}\end{pmatrix}.$$

The period coordinate of the superposition at the origin (0,0) will be, in this case, $(0, 0, -\frac{1}{2}, -\frac{1}{2})$. Clearly, if before the shift the plane Im(Ξ) contained integer points of $\mathbb{Z}^4$, then after this shift Im(Ξ) will contain none: the superposition will have no dot-centered rosettes.

Proposition 4: If grating $p_i(\mathbf{x})$ is shifted by an integer number of its periods, the superposition $p(\mathbf{x})$ and its microstructure remain, of course, unchanged. This is expressed in $\mathbb{R}^m$ by the fact that the plane Im(Ξ) is shifted along the ith axis of $\mathbb{R}^m$ by an integer number, so that the relative location of the plane with respect to points of $\mathbb{Z}^m$ remains unchanged. ■

Proposition 5: Assume that each of the individual gratings $p_i(\mathbf{x})$ is shifted by a noninteger number of periods. The combination of their shifts gives a rigid motion of the superposition as a whole (and hence only a lateral shift of the microstructure) *iff* these shifts cause the plane Im(Ξ) to be shifted into itself in $\mathbb{R}^m$ (or in other words: *iff* the plane Im(Ξ) is shifted within $\mathbb{R}^m$ by a vector which is included in this plane). ■

This result is easy to understand, since a rigid motion of the superposition by (x_0,y_0) implies that every point $(\xi_1,\ldots,\xi_m)$ which used to be in Im(Ξ) before the rigid transformation will still remain in Im(Ξ), but now it will correspond in the superposition to the point $(x,y)-(x_0,y_0)$ rather than to the point (x,y).

6 Microstructures in the Conventional Three-Screen Superposition

A particularly interesting case occurs in the conventional three-screen superposition used for color printing, i.e., the superposition of three identical dot screens (or square grids) with equal angle differences (for example, at orientations of $\theta_1=30°$, $\theta_2=-30°$, and $\theta_3=0°$). As we have seen in Sec. 3.2, in this case the in-phase superposition generates an almost-periodic pattern of dot-centered rosettes [see Fig. 6(b)]; but when one of the superposed layers is shifted by half a period in each of its two main directions, the microstructure of the superposition changes into a pattern of clear-centered rosettes [see Fig. 6(c)]. How can we explain this interesting phenomenon mathematically, using our new algebraic formulation? And why, as we have seen in Fig. 9, does this phenomenon not occur when only two of the three layers are superposed?

The transformation Ξ is defined for this three-layer in-phase superposition by

$$\Xi\begin{pmatrix}x\\y\end{pmatrix}=\begin{pmatrix}\xi_1\\\xi_2\\\xi_3\\\xi_4\\\xi_5\\\xi_6\end{pmatrix}=\frac{1}{T}\begin{pmatrix}M_{30}\begin{pmatrix}x\\y\end{pmatrix}\\M_{-30}\begin{pmatrix}x\\y\end{pmatrix}\\I\begin{pmatrix}x\\y\end{pmatrix}\end{pmatrix}=\frac{1}{T}\begin{pmatrix}\frac{\sqrt{3}}{2}x+\frac{1}{2}y\\-\frac{1}{2}x+\frac{\sqrt{3}}{2}y\\\frac{\sqrt{3}}{2}x-\frac{1}{2}y\\\frac{1}{2}x+\frac{\sqrt{3}}{2}y\\x\\y\end{pmatrix}, \tag{14}$$

where M_{30} and M_{-30} are the matrices which represent rotations by 30° and −30°, respectively, and I is the identity matrix

$$M_\theta=\begin{pmatrix}\cos\theta & \sin\theta\\-\sin\theta & \cos\theta\end{pmatrix}\quad I=M_0=\begin{pmatrix}1&0\\0&1\end{pmatrix}.$$

Transformation Ξ maps, therefore, the x,y superposition plane into a plane Im(Ξ) within $\mathbb{R}^6$. Note that except for the point (0,0,0,0,0,0) the plane Im(Ξ) contains no integer point of $\mathbb{Z}^6$, since, according to Eq. (14), whenever ξ_5 and ξ_6 are integers, ξ_1, ξ_2, ξ_3, ξ_4 are irrational numbers. This is not surprising, since we already know that our three-screen superposition is not periodic, but rather almost peri-

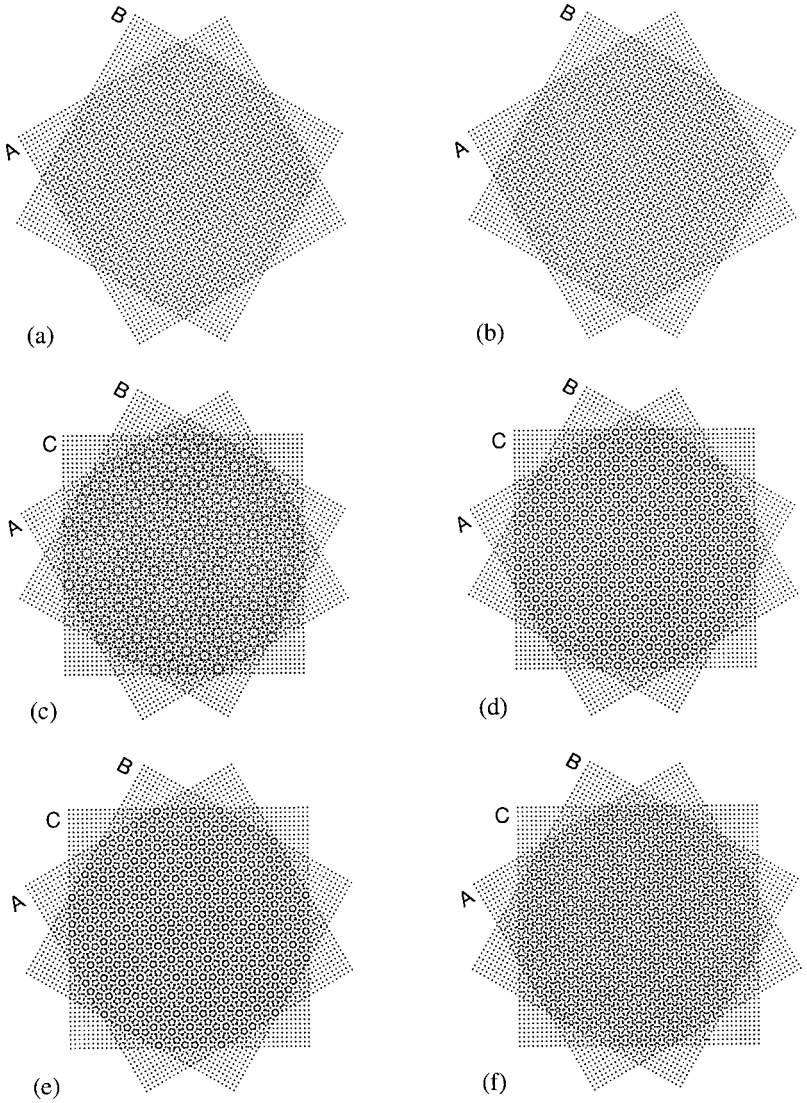

Fig. 12 (a) In-phase superposition of two identical dot screens at angles $\theta_1 = 30°$ and $\theta_2 = -30°$. (b) Counter-phase superposition of the same screens. (c) In-phase superposition of a third identical screen with angle $\theta_3 = 0°$ on top of (a); the period shifts of the screens are (0,0,0,0,0,0). (d) Counter-phase superposition of a third identical screen with angle $\theta_3 = 0°$ on top of (a); the period shifts of the screens are $(0,0,0,0,\frac{1}{2},\frac{1}{2})$. (e) Counter-phase superposition of a third identical screen with angle $\theta_3 = 0°$ on top of (b); the period shifts of the screens are $(\frac{1}{2},\frac{1}{2},\frac{1}{2},\frac{1}{2},\frac{1}{2},\frac{1}{2})$. (f) Half period shifted superposition of a third identical screen with angle $\theta_3 = 0°$ on top of (a); the period shifts of the screens are $(0,0,0,0,\frac{1}{2},0)$.

odic (in the language of Ref. 9: the six frequency-vectors $\mathbf{f}_1 = (\frac{\sqrt{3}}{2},\frac{1}{2})$, $\mathbf{f}_2 = (-\frac{1}{2},\frac{\sqrt{3}}{2})$, $\mathbf{f}_3 = (\frac{\sqrt{3}}{2},-\frac{1}{2})$, $\mathbf{f}_4 = (\frac{1}{2},\frac{\sqrt{3}}{2})$, $\mathbf{f}_5 = (1,0)$, and $\mathbf{f}_6 = (0,1)$ span within the u,v plane a module with rank$=4$, since $\mathbf{f}_1$, $\mathbf{f}_2$, $\mathbf{f}_3$ and $\mathbf{f}_4$ are linearly independent over $\mathbb{Z}$, but $\mathbf{f}_5 = \mathbf{f}_4 - \mathbf{f}_2$ and $\mathbf{f}_6 = \mathbf{f}_1 - \mathbf{f}_3$) (see note e in notes section).

In order to better understand the microstructure of the conventional three-screen superposition with equal angle differences of 30° (or 60°), let us return for a moment to the superposition of two identical screens with an angle difference of 30° (or 60°). As we have seen in Example 2 above and in Fig. 9, this superposition is characterized by the presence of approximate rosettes of all types (dot centered, clear centered, and all intermediate variants), which are uniformly distributed throughout the superposition plane, giving to the eye the impression of a uniform, regular microstructure. This situation is shown again in Fig. 12(a) and in its magnified version in Fig. 13(a). Figures 12 and 13 also show in detail what happens when we superpose the third dot screen on top of this two-screen superposition (keeping our convention that in the initial phase of each layer a black dot is centered on the origin):

1. If the third dot screen is superposed in phase with the first two screens, so that all screens have a black dot centered on the origin, then wherever there used to be in the two-screen superposition an almost-dot-centered rosette or an almost-clear-centered rosette, the third screen contributes a new dot of its own. This strengthens all the already

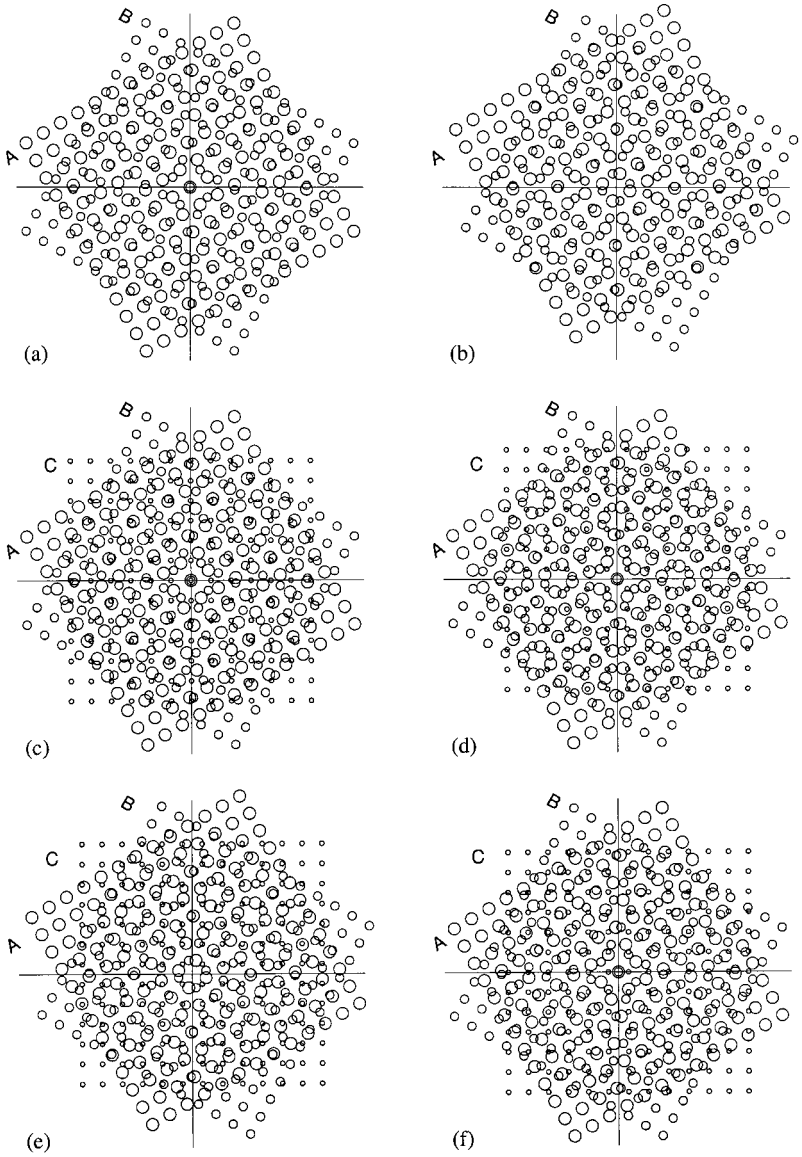

Fig. 13 A magnified view of the screen superpositions of Fig. 12, where the dots of each layer are represented by circles of a different size, thus permitting us to distinguish between the different layers and their precise dot locations.

existing dot-centered rosettes, but destroys all the two-screen clear-centered rosettes. As a result, the three-layer superposition no longer contains almost-clear-centered rosettes, and the microstructure becomes dominated by almost-dot-centered rosettes [compare the two layers in Figs. 12(a) and 13(a) with the three layers in Figs. 12(c) or 13(c), respectively].

2. If the third dot-screen is superposed in counter phase with respect to the first two screens, i.e., with a white space centered on the origin, then wherever there used to be in the two-screen superposition an almost-clear-centered rosette or an almost dot-centered rosette, the third screen contributes a white space (which is obviously surrounded by four black dots). This strengthens all the already existing clear-centered rosettes, but destroys all the dot-centered rosettes. As a result, the three-layer superposition no longer contains almost-dot-centered rosettes, and the microstructure becomes dominated by almost-clear-centered rosettes [compare the two layers in Figs. 12(a) and 13(a) with the three layers in Figs. 12(d) or 13(d), respectively].

3. If all of the three screens are centered on the origin in counter phase (i.e., with a white space centered on the origin), the addition of the third layer on top of the two-screen superposition has the same effect as in case (2) [compare the two layers in Figs. 12(b) and 13(b) with the three layers in Figs. 12(e) or 13(e), respectively].

As we can see, the addition of the third layer significantly modifies the microstructure behavior of the superposition: While in the two-screen superposition almost rosettes of all types are uniformly distributed throughout the plane, when the third layer is added on top, one type of almost rosettes becomes dominant. Furthermore, in contrast to the two-screen superposition, where shifts of the individual screens do not modify the nature of the microstruc-

ture [see Figs. 12(a) and 12(b)], in the three-screen superposition a shift of any of the layers may alter the dominant type of rosettes in the superposition and thus visibly modify the texture of the microstructure [see Figs. 12(c) to 12(f)].

Although this behavior may seem surprising at first sight, in fact, there is nothing mysterious about it. As we already know, the plane $\mathrm{Im}(\Xi)$ within $\mathbb{R}^4$ that contains all the period-coordinates $(\xi_1,\xi_2,\xi_3,\xi_4)$ of the two dot screens at 30° and −30° is irrational, and, therefore, it contains no integer points of $\mathbb{Z}^4$ except for (0,0,0,0)—but it passes within $\mathbb{R}^4$ as close as we wish to integer points of $\mathbb{Z}^4$ and to half integer points of $\mathbb{Z}^4+(\frac{1}{2},\frac{1}{2},\frac{1}{2},\frac{1}{2})$ (which correspond, respectively, to dot-centered or to clear-centered rosettes in the two-screen superposition). Now, when we superpose a new dot screen at 0° on top of the first two screens, we increase the dimension of the period-coordinate vectors by 2, from $(\xi_1,\xi_2,\xi_3,\xi_4)\in\mathbb{R}^4$ to $(\xi_1,\xi_2,\xi_3,\xi_4,\xi_5,\xi_6)\in\mathbb{R}^6$. Denoting by Ξ' the extension of the transformation Ξ to $\mathbb{R}^6$, it is clear that $\mathrm{Im}(\Xi')$ remains a 2D plane within the extended period-coordinate space $\mathbb{R}^6$, where the first four coordinates ξ_1, ξ_2, ξ_3, ξ_4 of each point are the same as in $\mathrm{Im}(\Xi)$ before. Let us see now what happens, for example, in case (a) above: In this case, wherever in $\mathbb{R}^4$ our plane $\mathrm{Im}(\Xi)$ was close (say, up to ε) to a half integer point, there come the two new coordinates ξ_5 and ξ_6 and destroy the candidacy of that point as an almost-half integer within $\mathbb{R}^6$. As we will show below, this happens since the two new coordinates ξ_5 and ξ_6 are *not independent* of their predecessors ξ_1, ξ_2, ξ_3, ξ_4: as can be seen from Eq. (14) above, for any point (x,y) in the superposition plane we have $\xi_5=\xi_4-\xi_2$ and $\xi_6=\xi_1-\xi_3$. Note that if $\xi_1,\ldots,\xi_6$ were all independent of each other, then some of the almost-half integer points in $\mathbb{R}^4$ would be, indeed, destroyed by ξ_5 and ξ_6, but infinitely many other almost-half integer points would still remain almost-half integer points in $\mathbb{R}^6$, too.

Let us see now how we can explain cases 1–3 above mathematically, using our new algebraic formulation.

Let us first consider the two superposed screens which are oriented to angles 30° and −30°. Assume at first that both screens have a black dot centered on the origin [see Fig. 12(a)]. Since the superposition of these two screens is almost periodic, at no point (x,y) in the superposition except for the origin a precise dot superposition may occur; but at infinitely many points (x,y) we have an almost-perfect dot superposition, where ξ_1, ξ_2, ξ_3, ξ_4 are almost integers, or an almost-perfect white space superposition, where ξ_1, ξ_2, ξ_3, ξ_4 are almost-half integers. Let (x,y) be such a point (of either type); this means, therefore, that at this point

$$\begin{pmatrix}\xi_1\\ \xi_2\end{pmatrix}-\begin{pmatrix}\xi_3\\ \xi_4\end{pmatrix}\approx\begin{pmatrix}m\\ n\end{pmatrix}\quad\text{where}\quad m,n\in\mathbb{Z},\tag{15}$$

namely

$$\frac{1}{T}\left[M_{30}\begin{pmatrix}x\\ y\end{pmatrix}-M_{-30}\begin{pmatrix}x\\ y\end{pmatrix}\right]\approx\begin{pmatrix}m\\ n\end{pmatrix},$$

$$\frac{1}{T}\left[\begin{pmatrix}\frac{\sqrt{3}}{2} & \frac{1}{2}\\ -\frac{1}{2} & \frac{\sqrt{3}}{2}\end{pmatrix}\begin{pmatrix}x\\ y\end{pmatrix}-\begin{pmatrix}\frac{\sqrt{3}}{2} & -\frac{1}{2}\\ \frac{1}{2} & \frac{\sqrt{3}}{2}\end{pmatrix}\begin{pmatrix}x\\ y\end{pmatrix}\right]\approx\begin{pmatrix}m\\ n\end{pmatrix},$$

$$\frac{1}{T}\begin{pmatrix}0 & 1\\ -1 & 0\end{pmatrix}\begin{pmatrix}x\\ y\end{pmatrix}\approx\begin{pmatrix}m\\ n\end{pmatrix},$$

$$\frac{1}{T}\begin{pmatrix}y\\ -x\end{pmatrix}\approx\begin{pmatrix}m\\ n\end{pmatrix},$$

and, therefore

$$\frac{1}{T}\begin{pmatrix}x\\ y\end{pmatrix}\approx\begin{pmatrix}k\\ l\end{pmatrix}\quad\text{with}\quad k,l\in\mathbb{Z}.\tag{16}$$

Now, if the third, 0° screen is superposed in phase [i.e., with a black dot centered on the origin, like in Fig. 12(c)], then Eq. (16) means (see note f in Notes section)

$$\begin{pmatrix}\xi_5\\ \xi_6\end{pmatrix}\approx\begin{pmatrix}k\\ l\end{pmatrix}\quad\text{with}\quad k,l\in\mathbb{Z}.\tag{17}$$

This shows, therefore, that at any point (x,y) in the superposition which satisfies condition (15), and in particular, at any point (x,y) where $\xi_1,\ldots,\xi_4$ are almost integers (giving a two-layer almost-dot-centered rosette) or almost-half integers (giving a two-layer almost-clear-centered rosette), the period-coordinates ξ_5, ξ_6 of the third, 0° screen are necessarily almost integer. This means that the third screen contributes to the superposition a black dot of its own very close to (x,y). This strengthens all the already existing dot-centered rosettes, but destroys all the two-screen clear-centered rosettes. As a result, the three-layer superposition no longer contains almost-clear-centered rosettes, and the microstructure becomes dominated by almost-dot-centered rosettes. This explains, indeed, case 1 above.

If, however, the third, 0° screen is superposed in counter phase with respect to the 30°- and the −30°-screens [i.e., with a white space centered on the origin, like in Fig. 12(d)], then we have from Eq. (16)

$$\begin{pmatrix}\xi_5\\ \xi_6\end{pmatrix}-\begin{pmatrix}\frac{1}{2}\\ \frac{1}{2}\end{pmatrix}\approx\begin{pmatrix}k\\ l\end{pmatrix}\quad\text{with}\quad k,l\in\mathbb{Z}.$$

This means that at any point (x,y) in the superposition where ξ_1, ξ_2, ξ_3, ξ_4 are almost integers (giving a two-layer almost-dot-centered rosette) or almost-half integers (giving a two-layer almost-clear-centered rosette), the period-coordinates ξ_5, ξ_6 of the third, 0° screen are necessarily almost-half integer, so that the third screen contributes a white-space centered very close to (x,y). This strengthens all the already existing clear-centered rosettes, but destroys all the dot-centered rosettes. As a result, the three-layer superposition no longer contains almost-dot-centered rosettes, and the microstructure becomes dominated by almost-clear-centered rosettes. This is, indeed, the explanation of case 2 above.

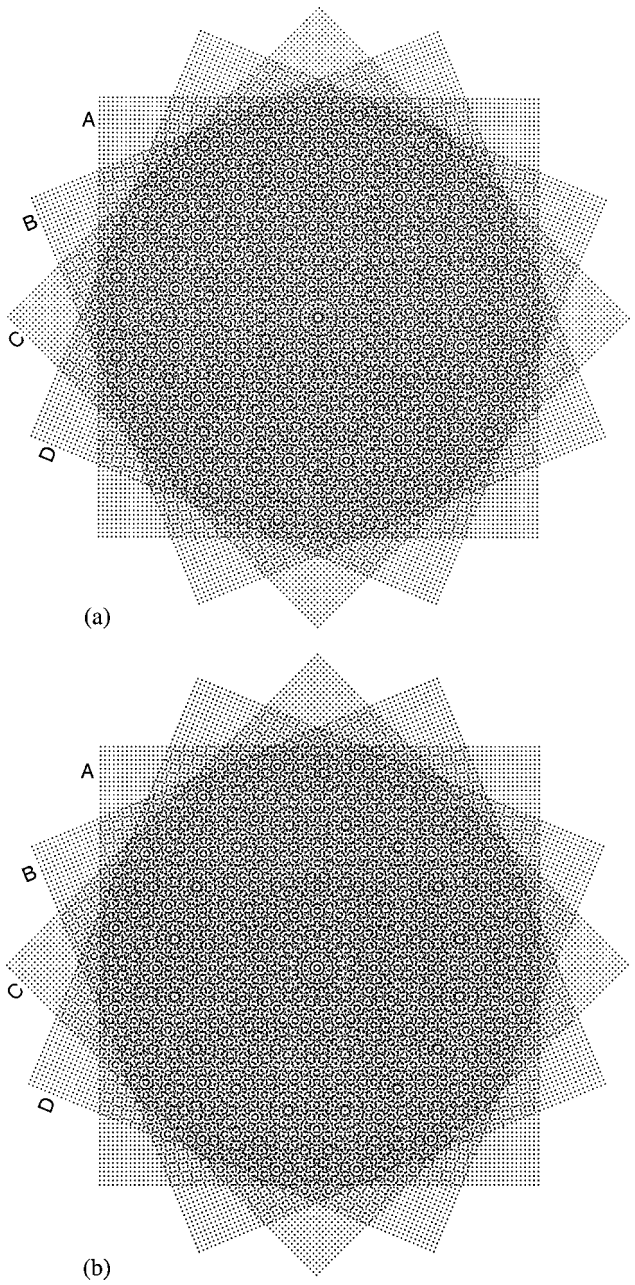

Fig. 14 The superposition of four identical screens with equal angle differences of 22.5°: (a) in-phase superposition; (b) counter-phase superposition.

Finally, in case 3, where the three screens are superposed with a white space centered on the origin, the demonstration remains the same as in case 2.

Note, however, that if the third screen were independent of the first two superposed screens, then the microstructure in the three-screen superposition would remain uniformly disordered and invariant under layer shifts, as in the original two-screen superposition.

7 Behavior of Microstructure Under Layer Shifts

As we can see, the microstructure of the conventional three-screen superposition is not invariant under shifts of the individual layers because in this case the superposed layers are not independent of each other. And indeed, whenever the superposed layers are independent—as in the case of the two-screen superposition at 0° and 30°—all types of almost rosettes are simultaneously present in the superposition, and no substantial microstructure changes occur when individual layers are shifted. Restated more formally, the superposition undergoes substantial microstructure changes under shifts of individual layers *iff* the superposed layers are dependent on each other, i.e., for some given integers k_i (not all zeroes) we have for all points $\mathbf{x}=(x,y)$ in the superposition $\Sigma k_i \xi_i = 0$.

It should be noted that during the discussion until now we considered the linear dependence (or independence) over $\mathbb{Z}$ of the scalars ξ_i. However, this is fully equivalent to the linear dependence (or independence) over $\mathbb{Z}$ of the frequency vectors $\mathbf{f}_i$, since: $\Sigma k_i \mathbf{f}_i = \mathbf{0} \Leftrightarrow \forall \mathbf{x}\ (\Sigma k_i \mathbf{f}_i)\cdot \mathbf{x} = 0 \Leftrightarrow \forall \mathbf{x}\ \Sigma k_i \mathbf{f}_i \cdot \mathbf{x} = 0 \Leftrightarrow \forall \mathbf{x}\ \Sigma k_i \xi_i = 0$ [by Eq. (9)]. We obtain, therefore, the following general result (see note g in Notes section):

Proposition 6: A nontrivial shift of individual layers in the superposition causes a substantial change in the microstructure of the superposition *iff* their frequency vectors $\mathbf{f}_i$ are linearly dependent over $\mathbb{Z}$, i.e., *iff* there exist $k_i \in \mathbb{Z}$ not all of them 0 such that $\Sigma k_i \mathbf{f}_i = \mathbf{0}$. But this precisely means that the superposition is *singular*. ■

Example 3: Let us illustrate this result with a few singular or nonsingular cases:

i. *A two-screen periodic, singular case:* The periodic two-screen superposition of Example 1 above is singular, and, therefore, layer shifts may cause substantial changes in its microstructure [see also Sec. 3.1 and Figs. 5(b) and 5(c)].

ii. *A three-screen almost-periodic, singular case:* The conventional three-screen superposition is singular, and, indeed, as we have seen above, layer shifts may cause substantial changes in its microstructure (see Fig. 6).

iii. *A two-screen almost-periodic, non-singular case:* A stable moiré-free two-screen superposition, like the superposition of two identical screens with angle difference of 30°, is nonsingular; therefore, its microstructure consists of a uniform blend of rosettes of all types, and it is not substantially influenced by layer shifts (see Fig. 9).

iv. *A three-screen almost-periodic, nonsingular case:* A stable moiré-free three-screen superposition, like the screen combination discussed in Ref. 11 (see Fig. 19 there), is nonsingular; therefore, its microstructure consists of a uniform blend of rosettes of all types, and it is not substantially influenced by layer shifts.

v. *A four-screen almost-periodic, nonsingular case:* The superposition of four identical screens with equal angle differences of 22.5° (see Fig. 14) is nonsingular. Therefore its microstructure consists of a blend of rosettes of all types, and it is not substantially influenced by layer shifts: Although each layer shift is distinct, all rosette types are equally represented in all the different layer shifts,

and there is no predominance of one particular rosette type in each layer shift. ■

It should be noted, however, that even when substantial microstructure modifications do occur, i.e., when the superposition is singular, they still may be more visible or less visible; but Proposition 6 does not say which cases give more significant or less significant modifications and why. In general, a moiré which is clearly visible with a strong amplitude has, by Propositions 1 and 2, significantly different in-phase and counter-phase microstructure. Therefore, when it becomes singular the microstructure variation (between in-phase and counter-phase rosettes) due to layer shifts will be clearly visible. However, the higher the order of the singular state, the less visible are its microstructure changes in the superposition, and, therefore, the rosette-type changes which arise due to layer shifts in the singular state (see Proposition 2) are almost unperceptible—although they do exist according to Proposition 6.

8 Summary

In the superposition of periodic layers such as dot screens, new structures may appear that did not exist in any of the original layers. These new structures may include both macrostructures (moiré effects) and microstructures (rosettes). But while microstructures exist practically in any superposition, except for the most trivial cases, macromoiré effects are not always present; and moreover, whenever they do exist, they are, in fact, built from the microstructures of the superposition.

In view of the important role of the microstructures in superpositions of periodic layers, we investigate their behavior and their properties both in the image domain and in the spectral domain. We first explore the behavior of the microstructure in the different types of singular and nonsingular superpositions. Then, we provide an algebraic formalization which gives us the mathematical tools for understanding the various properties of the microstructures. This formalization also leads us to new, general results concerning the stability of the microstructure under layer shifts in the superposition. In particular, we show that shifts of individual layers substantially change the microstructure of the superposition *iff* the superposition is singular.

Remark: Parts of this manuscript have been used for preparing Chapter 8 in Ref. 14.

Notes

a. Obviously, the period of the microstructure is always greater than or equal to the original screen periods: Since the impulses of the original screen frequencies $\mathbf{f}_i$ are included in the compound nail bed, it is clear that the fundamental impulses of the compound nail bed can either coincide with the original screen frequencies $\mathbf{f}_i$, or fall even closer to the dc [as in the $(1,2,-2,-1)$ moiré; see Fig. 5(a)].

b. Singular states in which there is no clear visual distinction between in-phase and counter-phase microstructures do not produce off the singular state a visible macromoiré in the superposition. This often happens in moirés of high orders, or in moirés involving many superposed layers.

c. It is interesting to note that if the superposition in the (x,y) plane consists of nonlinearly curved layers (i.e., nonlinear transformations of periodic functions; see Ref. 13), then the image of Ξ is a curved 2D surface within $\mathbb{R}^m$.

d. More precisely: for any positive ϵ, be it as small as we may desire, we can find in the superposition rosettes (or either type) with a mismatch smaller than ϵ, provided that we go far enough from the origin.

e. It is interesting to note that the superposition of the third screen on top of the initial two-screen superposition does not add new impulse locations in the spectrum support [compare the two-screen spectrum support in Fig. 9(a) with the three-screen spectrum support in Fig. 6(a)]. The reason is that the new frequency vectors $\mathbf{f}_5$ and $\mathbf{f}_6$ are linear combinations of the original frequency vectors $\mathbf{f}_1$, $\mathbf{f}_2$, $\mathbf{f}_3$, $\mathbf{f}_4$, and therefore, all the new convolution impulses which are generated in the spectrum owing to the superposition of the third screen are located on top of already existing impulses. Thus, each impulse in the spectrum of the two-screen superposition turns into a *compound impulse* in the spectrum of the three-screen superposition, and the nonsingular two-screen superposition turns into a singular three-screen superposition.

f. Note that if one already observed from Eq. (14) that $\xi_5=\xi_4-\xi_2$ and $\xi_6=\xi_1-\xi_3$, then Eq. (17) can be directly deduced from Eq. (15).

g. Another interesting result of this equivalence is that, just as the spectral interpretation of a $(k_1,\ldots,k_m)$-singular superposition is $\Sigma k_i\mathbf{f}_i=0$, its image-domain interpretation is that, for any point $\mathbf{x}$ in the x,y plane, $\Sigma k_i\xi_i=0$ (provided that all the superposed layers are given in their initial phase). For example, in Fig. 10, which illustrates a $(1,2,-2,-1)$-singular superposition, any point $\mathbf{x}$ in the x,y plane satisfies: $\xi_1+2\xi_2-2\xi_3-\xi_4=0$. (In the spectral domain we have, of course, $\mathbf{f}_1+2\,\mathbf{f}_2-2\,\mathbf{f}_3-\mathbf{f}_4=\mathbf{0}$.)

References

1. J. A. C. Yule, *Principles of Color Reproduction*, Chap. 13, pp. 328–345, Wiley, New York (1967).
2. K. Patorski, *Handbook of the Moiré Fringe Technique*, Elsevier, Amsterdam (1993).
3. *Selected Papers on Optical Moiré and Applications*. SPIE Milestone Series, Vol. MS64, G. Indebetouw and R. Czarnek (Eds.), SPIE Optical Engineering, (1992).
4. P. A. Delabastita, ''Screening techniques, moiré in color printing,'' *Proc. of the Technical Association of the Graphics Arts*, pp. 44–65 (1992).
5. K. Daels and P. Delabastita, ''Color balance in conventional halftoning,'' *Proc. of the Technical Association of the Graphics Arts*, pp. 1–18 (1994).
6. R. N. Bracewell, *The Fourier Transform and its Applications*, 2nd ed. McGraw–Hill, New York (1986).
7. R. Ulichney, *Digital Halftoning*, pp. 79–84, MIT, Cambridge, MA (1988).
8. I. Amidror, ''A generalized Fourier-based method for the analysis of

2D moiré envelope forms in screen superpositions,'' *J. Mod. Opt.* **41**, 1837–1862 (1994).
9. I. Amidror and R. D. Hersch, ''Analysis of the superposition of periodic layers and their moiré effects through the algebraic structure of their Fourier spectrum,'' *J. Math. Imaging Vision* **8**, 99–130 (1998).
10. I. Amidror and R. D. Hersch, ''Fourier-based analysis of phase shifts in the superposition of periodic layers and their moiré effects,'' *J. Opt. Soc. Am. A* **13**(5), 974–987 (1996).
11. I. Amidror, R. D. Hersch, and V. Ostromoukhov, ''Spectral analysis and minimization of moiré patterns in colour separation,'' *J. Electron. Imaging* **3**, 295–317 (1994).
12. M. Vygodski, *Aide-Mémoire de Mathématiques Supérieures*, Mir, Moscow (1973) (in French).
13. I. Amidror and R. D. Hersch, ''Fourier-based analysis and synthesis of moirés in the superposition of geometrically transformed periodic structures,'' *J. Opt. Soc. Am. A* **15**(5), 1100–1113 (1998).
14. I. Amidror, *The Theory of the Moiré Phenomenon*, Kluwer, Dordrecht (2000).

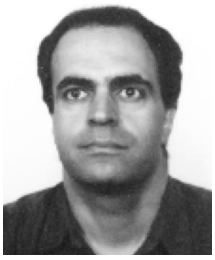

Isaac Amidror received his BS degree in mathematics from the Hebrew University of Jerusalem, Israel, and his MS degree in computer science from the Weizmann Institute of Science in Rehovot, Israel. He received a Japanese government scholarship for a two-year research perios in the Computer Science Department of the Toyohashi University of Technology in Japan. After having worked a few years in industry (notably in the fields of laser printing and digital typography), he received his PhD degree at the Swiss Federal Institute of Technology, in Lausanne, Switzerland. He has published numerous scientific papers and is the author of a recent book on the teory of the moiré phenomenon (http://lspwww.epfl.ch/books/moire/). His research interest include the mathematical foundation of moiré phenomena, document security, color image reproduction, image processing and digital typography.

Roger D. Hersch is a professor of computer science and head of the Peripheral Systems Laboratory at the Ecole Polytechnique Fédérale de Lausanne. He received his engineering and PhD degrees respectively from ETH Zurich in 1975 and the EPFL in 1985. He has published over 100 scentific papers, is the editor of 4 books, and is inventer or co-inventer in sceral patent applications. The lab's research is focussed on novel imaging techniques (color prediction, color reproduction, artistic imaging, anti-counterfeiting) and high-performance server applications (imaging servers, Web servers, PC clusters, etc._ He directs the Visible Human Web Server project, which offers advanced visualization services for exploring human anatomy (see http://visiblehuman.epfl.ch).